



4E and Multi-criteria Optimization of a New Alternative Intercooling Method for Modified Brayton Cycle on the Operation of a Hybrid Energy System

Vahab Okati¹ · Ali Jabari Moghadam¹ · Mahmood Farzaneh-Gord² · Mahbod Moein-Jahromi³

Received: 4 April 2023 / Accepted: 25 August 2023
© The Author(s), under exclusive licence to Shiraz University 2023

Abstract

Modifying a simple Brayton cycle by utilizing an intercooler/reheater during compression/expansion processes within the compressor/turbine is an enviro-economic feasible approach for a more efficient system with cleaner productions. A Brayton-Rankine cycle performance is enhanced in this study by placing an ejector refrigerating cycle (ERC) to produce refrigerating load from wasted heat recovery for the intercooling process between the compression stages in the Brayton cycle. Analyses including energy, exergy, economics, and environmental are performed to investigate the proposed combination of the Brayton-Rankine cycle with the ERC and compare it with various typical types of the Brayton-Rankine cycles. Eventually, a robust parametric study and multi-criteria optimization model are developed based on the non-dominated sorting genetic algorithm II method to assess system performance and find its optimal operating point. Results showed that the intercooler with cooling fluid coming from the ERC reduces the fuel consumption, CO₂ emission, and combined cycle's levelized cost of electricity (LCOE) significantly compared to common intercoolers with atmospheric air as the cooling fluid. The energy and exergy efficiencies of the proposed cycle are higher than the typical Brayton-Rankine cycles. The highest thermal and exergy efficiencies and the lowest fuel consumption, LCOE, and CO₂ emissions are 62.79%, 60.11%, 114.7 kg/MWh, 27.61 \$/MWh, 316.83 kg/MWh, respectively, related to the combination of the ERC and the reheat Brayton-Rankine cycle. These values are obtained through stand-alone technical and economic analyses. Applying simultaneous effects of exergy and economic indices in multi-objective optimization resulted in the optimum exergy efficiency of 57.64% and LCOE of 29.93 \$/MWh.

Keywords Energy efficiency · Power plant · Environmental analysis · Heat recovery · Thermo-economic analysis · Exergy efficiency

List of symbols

A Area (m²)
 C_p Specific heat at constant pressure (kJ/kg K)

\dot{C} Cost rate (\$)
 CRF Capital recovery factor (–)
 ex Specific exergy (kJ/kg)
 $\dot{E}x_{des}$ Exergy destruction rate (kW)
 $\dot{E}x$ Exergy rate (kW)
 h Specific enthalpy (kJ/kg)
 i_{eff} Effective annual cost of interest rate (%)
 LHV Lower heating value (kJ/kg)
 $LCOE$ Levelized cost of electricity (\$/MWh)
 \dot{m} Mass flow rate (kg/s)
 N Number of the system operating years
 P Pressure (kPa)
 ΔP Pressure drop (bar)
 \dot{Q} Heat rate (kW)
 R_{AC} Air compressor pressure ratio (–)

✉ Ali Jabari Moghadam
alijabari@shahroodut.ac.ir

Vahab Okati
vahab_okati@yahoo.com

Mahmood Farzaneh-Gord
m.farzanehgord@um.ac.ir

Mahbod Moein-Jahromi
mmoein@jahromu.ac.ir

- ¹ Faculty of Mechanical Engineering, Shahrood University of Technology, Shahrood 361995161, Iran
- ² Department of Mechanical Engineering, Ferdowsi University of Mashhad, 91775-1111, Mashhad, Iran
- ³ Department of Mechanical Engineering, Jahrom University, 74135-111, Jahrom, Iran

t	Operating time in a year (s)
T	Temperature (K)
T_{pz}	Primary zone combustion temperature
v	Velocity (m/s)
\dot{W}	Power rate (kW)
X	Mole fraction
Z	Purchase cost (\$)
\dot{Z}	Annual cost rate (\$/y)

Subscripts

a	Air
av	Average
AC	Air compressor
ch	Chemical
cond	Condenser
CC	Combustion chamber
D	Diffuser section of the ejector
DWH	Domestic water heater
e	Outlet
env	Environment
eva	Evaporator
f	Fuel
FWP	Feed water pump
g	Exhaust gas
gen	Generator
GT	Gas turbine
HE	Heat exchanger
HP	High pressure
i	Inlet
is	Isentropic
LP	Low pressure
MF	Mixed flow
mixing	Mixing section of the ejector
n	Nozzle
ne	Nozzle exit
net	Net output
ni	Nozzle inlet
ph	Physical
Q	Heat
RG	Regenerator
SF	Secondary flow
st	Steam
ST	Steam turbine
th	Thermal
tot	Total
W	Work

Greek symbols

ε	Heat exchanger effectiveness (%)
η	Efficiency (%)
γ	Specific heat ratio (–)
φ	Maintenance factor (–)
λ	Fuel to air ratio (–)
μ	Entrainment ratio (–)

τ	Residence time (s)
ρ	Density (kg/m ³)
ζ_{CO_2}	Levelized CO ₂ emission (kg/MWh)

Abbreviations

4E	Energy-Exergy-Economic-Environmental
AC	Air compressor
AP	Approach point
ARC	Absorption refrigeration cycle
BC	Brayton cycle
CC	Combustion chamber
CCHP	Combined cooling, heating, and power
CPER	Combined power and ejector refrigeration
DWH	Domestic water heater
ERC	Ejector refrigeration cycle
GA	Genetic algorithm
HRSG	Heat recovery steam generator
NSGA-II	Non-dominated sorting genetic algorithm II
ORC	Organic Rankine cycle
PP	Pinch point
RBC	Regenerative Brayton cycle
FC	Fuel consumption
ST	Steam turbine
TIT	Gas turbine inlet temperature

1 Introduction

The population and economic development are the most critical factors in the energy demand jump over the past decades. It leads the researchers to propose and design more efficient, sustainable, and eco-friendly power plants (Dang et al. 2023; Ge et al. 2022). While electricity generation is responsible for close to 40% of the global CO₂ emissions produced by the energy sector, the other 60% is generated primarily through fossil fuels in industry, heating in buildings, and transport (IAEA, International Atomic Energy Agency). Accordingly, increasing the efficiency of fossil fuel power plants (especially the Brayton cycles: BCs) is one of the exciting topics in this context.

The combustion chamber, compressor, turbine, and electric generator are parts of a gas turbine's standard base cycle (Durmusoglu et al. 2017). The latter can be combined with other cycles, such as Rankine and Erickson, to increase efficiency (Seyfour et al. 2022). Adding regeneration, intercooler compression stages (Xu et al. 2022), and reheated expansion stage (Kilani et al. 2019) are other methods used to develop and increase the efficiency of the Brayton cycle (BC) (Farmani and Manjili 2022).

The gas turbine's high outlet temperature enables its base cycle efficiency to be increased by using such developed bottoming cycles as the combined cooling-heating-power

(CCHP) (Kialashaki 2018), combined heating-power (CHP) (Raghavendra et al. 2022), and combined cooling-power (CCP) and so on to absorb the output wasted heat from the exhaust (Schall and Hirzel 2012).

Since the “Carnot Cycle” is ideal for power generation, the effort is made to direct all other cycles towards it to have the highest thermal efficiency of power generation cycles (Sheykhi et al. 2020) through isothermal compression and expansion processes or intercooling in the compression and reheating in the expansion processes.

Saidi et al. (2000, 2002) showed that using intercoolers to increase the efficiency of power plant cycles up to at least 200 MW is essential for most future systems. Mohammadi et al. (2019) concluded that increasing the number of further recoveries, intercooler, and reheating stages will reduce the specific CO₂ emission, leveled electricity costs, and specific fuel consumption and increase the thermal efficiency in a hybrid solar tower BC (Golbaten Mofrad et al. 2020). In Gas Turbine Emissions (2013), the authors showed that using an intercooler between the low and high-pressure compressor sections in marine motors or gas turbines increased the whole cycle's thermal efficiency and gave Rolls Royce WR-21 LMS-100 (in marine engines) and GE LM6000 SPRINT (in gas turbines; with an increase of up to 45%) as some examples.

Sanjay (2011) showed that adopting a multi-pressure-reheat steam generator configuration would minimize the cycle's exergy degradation by studying the compressor pressure-to-turbine inlet temperature ratio variations on the combined gas-steam cycle efficiency. Studying the regenerative inter-cooled-reheat BC, Tyagi et al. (2006) showed that intercoolers increased the thermal efficiency of gas turbines' base cycles and reported the optimum pressure-to-cycle inlet temperature ratio for its maximum value. Besides such important parameters as the performance, air temperature rise, freezing conditions due to severe winter, fan load factor, and heat load variations that have sometimes posed serious challenges for using air-cooled heat exchangers as intercoolers in the BC, the environmental effects of using such exchangers have also recently attracted attention (He et al. 2013; Li et al. 2018). Power plant cycles need compact, inexpensive intercoolers, whereas current types are usually conventional gas-to-liquid heat exchangers that are very bulky and expensive. Since the air resistance in their air side is generally predominant, the first step in designing and developing them is considering their thermal-hydraulic performance. The reheat cycle that includes two turbines with a combustion chamber before each and increases the shaft output power by about 35% (Wu et al. 1996) is another suitable method to increase the BC's efficiency (Gülen et al. 2020). Using a reheater in the new GT-9 gas turbine cycle, the ABB (Swiss factory) has expanded its efficiency from 32 to 40.5% (Schobeiri 2018). Cengel and Boles (2006) believed that since separate use

of reheating and intercooling equipment reduced BC's thermal efficiency, the simultaneous use of intercooling, reheating, and regenerating would also increase it. Ghadikolaie et al. (2023) developed a 4E parametric analysis to investigate the improvement of an available BC-based combined power plant located in Neka city, Iran. The power plant was based on the combination of gas and steam cycles, and the authors proposed the exhaust recovery to run two water desalination units. They stated that applying this proposal led 8.4% reduction in energy costs. Haloi and Gogoi (2022) assessed the impact of ionized combustion products of a magneto hydrodynamics BC on the performance of a combined energy system. They utilized the second law of thermodynamics for the system evaluation and found that the combustion chamber has the highest exergy destruction rate. Anvari et al. (2020) presented exergoeconomic and environmental models of a novel multi-generation energy system that can produce cold, heat, power, and freshwater. They developed a parametric study and concluded that the inlet temperature of the gas turbine has the highest impact on system performance. In another study, a new tri-generation waste-to-energy system was proposed and optimized by Ebrahimi-Moghadam and Farzaneh-Gord (2023). The system comprised a biomass-fired GTC and a double-effect absorption refrigeration cycle (ARC). To make their proposal applicable, they assessed the construction feasibility of utilizing the system for a case study in Iran. Wang et al. (2018) introduced two modifications of the GTC and utilized its exhaust for running an absorption refrigeration cycle (ARC). Moghimi et al. (2018) introduced a hybrid energy plant to simultaneously produce cold, heat, and power in an integrated system. Their system was based on heat recovery from an RBC to run an ORC and an ejector refrigeration cycle (ERC). Mohammadi et al. (2017) applied thermodynamics laws and prepared a sensitivity analysis to evaluate a new CCHP system configuration. The system comprises a BC, an ORC, and an ARC, and their results showed that it could produce 30 kW, 8 kW, and 7.2 tons of power, cooling, and hot water, respectively. Xu et al. (2015) developed a mathematical formulation of the CCHP plant composed of supercritical CO₂ gas turbine and ejector cycles. Comparing the outputs of their proposed modified model with the base one illustrated that the exergy efficiency was 22.5% higher in the modified model.

Surveying the available literature illustrates that those different kinds of hybrid energy systems could be found based on the recovery of exhaust gases of BCs. Also, additional changes have been applied to the primary BC to improve its performance.

Refrigeration cycles are commonly used in many hybrid power plants (CCP or CCHP systems) and simple cycles (Brayton or the Brayton-Rankine cycles) to generate cooling loads for air conditioning or cooling of

power plant equipment. Evaporative cooling, Fogging, Vapor-Compression Refrigeration Systems, Air-Standard Refrigeration Systems, Absorption – Refrigeration Systems (ARSs), and Multi-stage Refrigeration Cycles are among the refrigeration cycles used in the power generation cycle (Kakkirala and Velayudhan Parvathy 2022). The BC compressor usually consumes Two-thirds of the cycle's total input energy. Cooling (reduced temperature) of the compressor's compressed air in one or more stages minimizes the work required by the compression process. The compressor outlet's reduced temperature increases the inlet temperature of the gas turbine, and both increase the BC efficiency.

"Ejector" is another refrigeration cycle with advantages like low cost, lack of moving parts, resistance against corrosion and wear, and ease of construction. Studying solar-driven combined power and ejector refrigeration (CPER) systems, Ahmadzadeh et al. (2017) concluded that using the genetic optimization algorithm can reduce the system's thermal and exergy efficiencies by 25.5 and 21.27%, respectively. Liang et al. (2020) studied the heat recovery system in an internal combustion engine, launched a combined supercritical CO₂ power and transcritical CO₂ refrigeration cycles, and increased the system efficiency.

Vutukuru et al. (2019) showed that if ejectors were used in the solar-assisted transcritical CO₂-based tri-generation system, the COP of the whole system would be equal to 0.8. Studying geothermal-driven tri-generation systems consisting of conventional RC and ERC, Takleh and Zare (2021) showed that their proposed system's levelized product cost was 28.51 \$/GJ under summer conditions.

Ameri et al. (2010) studied a tri-generation system based on a micro-gas turbine with a steam ERC; they reported that using the CCHP system would cause 23% fuel savings in summer and 33% in winter, compared to when electricity, heat, and refrigeration were produced separately. Zhang et al. (2021) showed that in the parallel type ORC and ejector heat pump combined cycle, the system's output power and exergy efficiencies were 4.62 and 30.76% more than the base ORC, respectively.

Sun et al. (2014) studied the combined heat and power (CHP) based on ejector heat exchangers and absorption heat pumps and concluded that the new system's heating capacity was 41% more than its base cycle. Many studies (e.g., Alexis 2007; Galindo et al. 2019) have used a combination of refrigeration cycles to improve the efficiency of power cycles. Despite all the studies on increasing the Brayton base cycle's efficiency, many scientists still try to provide efficient, inexpensive, nature-friendly methods for the same purpose, and the trend is expanding rapidly. Nowadays, as energy, exergy, environment, and economics are the four areas evaluated in most scientific reports on thermodynamic cycles (Wang et al. 2022c), this paper has also explored the Brayton-Rankine cycle configuration from these points of

view. However, there is still a gap in utilizing modified BC versions in hybrid power plants because those used in most hybrid systems are simple types (Vazini Modabber and Kho-shgoftar Manesh 2021).

All BCs typically use compact, air-cooled heat exchangers (so-called dry) or rarely wet types as intercoolers between the two compression stages. As mentioned before, in using compact air-cooled heat exchangers as BC intercoolers, the environmental effects of their use have also been recently attended to, besides challenges regarding their essential design parameters. In compact air-to-air and gas-to-liquid heat exchangers, there is usually a pressure drop in the air side and a temperature rise in the intercooler's outlet compared to the air inlet to the first compression stage, reducing the BC efficiency. Problems mentioned about using air-cooled heat exchangers as intercoolers in power plant cycles have caused a day-to-day expansion of studies on intercoolers' improvements to increase the efficiency of power plant cycles and reduce fuel consumption to lower the pollutants' entry into the atmosphere. To overcome the defects caused by the conventional intercooling processes utilized in the BC, this study proposes a new idea based on the waste heat recovery (WHR) approach. This study has used the gas turbine's recycled wasted heat to start an ERC (which is the supplier source of the refrigerant load required by the intercooler between two compression stages in the Brayton-Rankine power cycle's intercooler combined regenerated heat (ICRH)) to increase the system's energy and exergy efficiencies. Further, it has shown the difference between the studied and other conventional power plant cycles by reducing fuel consumption and environmental impacts and increasing the cycle efficiency. Although using the ERC (Mohammed et al. 2022) is quite common in CCHP and CCP systems to generate cooling load, this study has used this load to reduce the outlet temperature of the first stage of the BC density. In a nutshell, the application of this proposal is to improve the techno-economic performance of conventional gas-steam power plants by utilizing an ERC for the intercooling process of the BC. Considering the mentioned gaps in the state-of-the-art and also the described motivations, the following novelties and objectives are to be sought in the present paper:

- Designing a new intercooling technique between the compression stages of the Brayton cycle, based on the ejector refrigerating cycle (ERC) combined with the Brayton-Rankine cycle to recover the wasted heat and generate the required refrigerating load (as far as the authors know, previous studies investigated the capability of producing refrigerating loads by the ERC and Brayton-Rankine power cycles combination just for external utilization such as air-conditioning, not reusing as an

intercooler for the compression process within the BC that has been proposed in this paper for the first time)

- Performing energy, exergy, economics, and environmental analyses (4E analyses) of the proposed combination of the ERC with the Brayton-Rankine cycle and comparing them with the traditional air-intercooling Brayton-Rankine cycles
- Developing a robust technical assessment model by considering fluid flow and heat transfer phenomenon inside important system components (despite most research which treated the components as black boxes) and their combination with thermodynamics laws. Factual assumptions and detailed formulation are used to analyze the intercooler, ejector, and combustion chamber.
- Performing a multi-criteria optimization procedure based on the non-dominated sorting genetic algorithm II (NSGA-II) method.

To meet the mentioned goals, the rest of the paper is planned to be presented in four sections, including (a) Sect. 2 focuses on describing the system under study and its operating strategy, (b) Sect. 3 pays attention to developing the 4E parametric model, and the optimization method, (c) Sect. 4 presents the results and gives some discussion around them, (d) Sect. 5 summarizes the studied problem and the most important general findings.

2 System Description

As mentioned in the present investigation, an innovative configuration of a hybrid energy system is proposed to solve the problems caused by the conventional intercooling process in the BC. The schematic layouts of the conventional gas-steam combined power plant and the proposed system are depicted in Fig. 1a and b, respectively. These power systems include the modified BC and RC, which combine to form a hybrid power generation system. The BC includes an intercooler, reheater, and regenerator. The main difference in cycles 1-a and 1-b is in the cooling in the intercooler section. An air-cooled type is used in the first cycle, while the second system uses an ERC as the intercooler. Heat return from HRSG and heat transfer with the generator in a combined ejector system will reduce pump power consumption and increase efficiency in the intercooler section. Further explanations will be provided. The operation of the system can be described as follows.

The air is first sucked by compressor 1, and after an increase in pressure and temperature increases, it enters the intercooler. Then, passing through the intercooler, to maintain the compressor's efficiency and optimal working conditions, the air cools down and enters compressor 2. Afterward, the air enters the regenerator to receive the

wasted heat of the gas turbine exhaust. It is then injected into the combustion chamber, and the air and fuel react and reach very high temperatures. As the temperature increases, the pressure also increases, and the output combustion products enter the first stage of the gas turbine and, after a reduction of pressure, are reheated to increase its pressure and then enter the second stage of the gas turbine. This intermediate heating increases the power output by the turbine for the same pressure ratio. Finally, the combustion products enter the HRSG after heat transfer in the regenerator. In HRSG, waste heat is given to water to generate steam. This superheated steam then enters the steam turbine, and after generating power by the turbine, a pressure drop occurs and enters the condenser in order to condense the fluid. It is then pumped back into the HRSG to complete the cycle.

The combustion gas enters the ERC in the second cycle after passing through HRSG. The liquid refrigerant is pumped to the generator operating pressure in the ERC. The refrigerant enters the generator, converts to vapor, and leaves the generator as a saturated vapor. The vapor from the generator enters the convergent-divergent nozzle of the ejector, and its velocity increases while the pressure decreases in the diffuser throat. This flow is known as primary flow. At the nozzle output, the immediate flow creates a low-pressure zone that causes the secondary flow to be sucked out of the intercooler. The primary and secondary flows are mixed, and the mixture pressure is increased by the diffuser and then fed into the condenser. The task of the ejector is to convert work (i.e., pressure) to kinetic energy (i.e., velocity). The schematic diagram of this process within the ejector is illustrated in Fig. 2. The ejector includes four sub-components: nozzle, mixing chamber, throat, and diffuser. A parameter is the mass entrainment ratio of the ejector (μ) and is defined as the ratio of the mass flow rates of the secondary flow (SF) to the primary flow (PF).

By maintaining the pressure, the work of the pump is reduced. Some of this condensed liquid passes through the expansion valve. The pressure drops drastically as the dense liquid passes through the expansion valve. As the pressure drops, its temperature also drops drastically and enters the intercooler to cool the hot air. The rest is returned to the generator by the pump. Finally, the T-s diagram for different sub-cycles of the proposed system is drawn in Fig. 3.

3 Governing Equations and Solution Procedure

3.1 Energy Analysis

To evaluate the performance of an energy system, the mass and energy analyses of all system components must first be examined, which are written by the following equation,

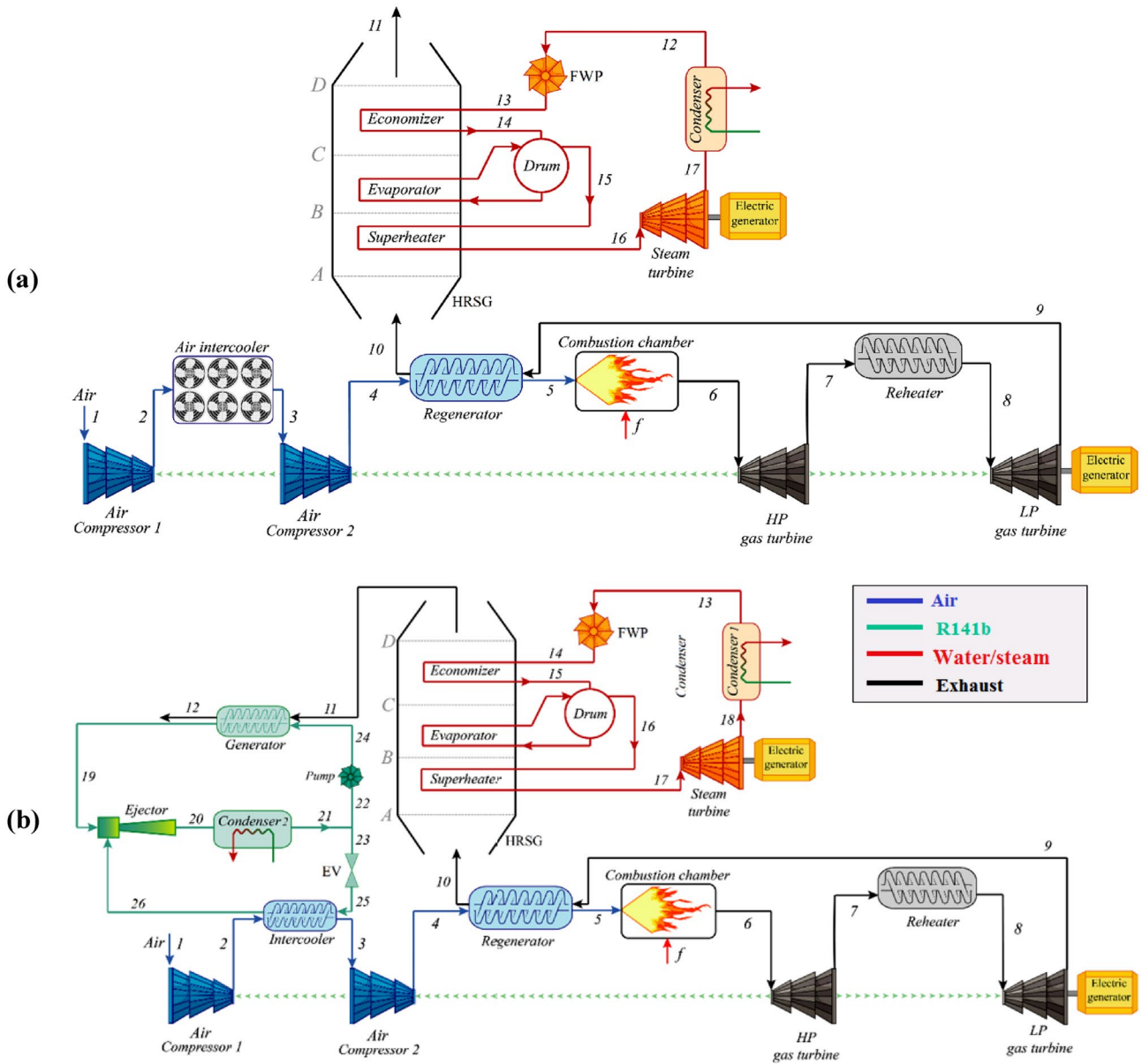


Fig. 1 Schematic sketch of the **a** system 1: combined regenerated inter-cooled reheat Brayton and Rankine power cycle, **b** system 2: proposed CCHP cycle configuration (the ERC is replaced with the air intercooler of the system 1)

regardless of the changes in kinetic and chemical energy under steady-state conditions (Musharavati et al. 2021).

$$\left(\sum \dot{m}_{in}\right) - \left(\sum \dot{m}_{out}\right) = 0 \quad (1)$$

$$\left(\sum \dot{m}_{in}h_{in}\right) - \left(\sum \dot{m}_{out}h_{out}\right) + \dot{Q} - \dot{W} = 0 \quad (2)$$

\dot{W} , \dot{Q} , z , g , v , h , and \dot{m} represent mechanical power, thermal power, altitude, gravity acceleration, velocity, enthalpy, and mass flow rate, respectively. Also, the 'in' and 'out' subtitles are related to the input and output currents to the control volume, respectively. The following is a detailed description of the modeling of each subsystem.

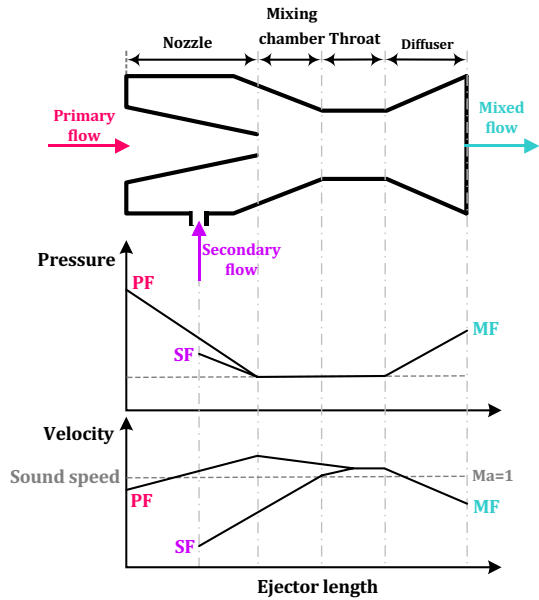


Fig. 2 A schematic view of an ejector and variation of pressure and velocity inside it

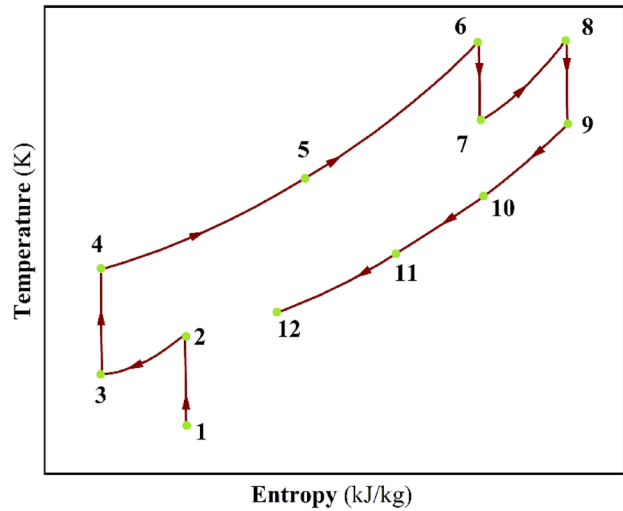


Fig. 3 T-s diagram of the regenerated inter-cooled reheat Brayton cycle

Table 1 Energy balance equations for components of the modified RBC

Component	Governing equations	Description
Air compressor 1	$T_2 = T_1 \times \left(1 + \frac{1}{\eta_{AC}} \left(R_{AC}^{\frac{\gamma_a-1}{\gamma_a}} - 1 \right) \right)$ $\dot{W}_{AC,1} = \dot{m}_a \int_{T_1}^{T_2} C_{p_a} dT$ $C_{p_a}(T) = 1.048 - \left(\frac{1.83T}{10^4} \right) + \left(\frac{9.47T^2}{10^7} \right) - \left(\frac{5.49T^3}{10^{10}} \right) + \left(\frac{7.92T^4}{10^{14}} \right)$	\dot{m}_a represents the air mass flow rate, $\eta_{AC} = 0.85$ is isentropic efficiency, and C_{p_a} is the specific heat at constant pressure (Ahmadi et al. 2011; Valero et al. 1994)
Air compressor 2	$T_4 = T_3 \times \left(1 + \frac{1}{\eta_{AC}} \left(R_{AC}^{\frac{\gamma_a-1}{\gamma_a}} - 1 \right) \right)$ $\dot{W}_{AC,2} = \dot{m}_a \int_{T_3}^{T_4} C_{p_a} dT$ $C_{p_a}(T) = 1.048 - \left(\frac{1.83T}{10^4} \right) + \left(\frac{9.47T^2}{10^7} \right) - \left(\frac{5.49T^3}{10^{10}} \right) + \left(\frac{7.92T^4}{10^{14}} \right)$	Ahmadi et al. (2011), Valero et al. (1994)
Air intercooler	$\dot{Q}_{int} = \dot{m}_a (h_2 - h_3)$	
Regenerator	$\dot{m}_a (h_5 - h_4) = \dot{m}_g (h_{10} - h_9)$ $\frac{P_5}{P_4} = (1 - \Delta P_{RG})$ $\epsilon_{RG} = \frac{T_5 - T_4}{T_9 - T_4}$	$\epsilon_{RG} = 81\%$ is the regenerator effectiveness, and ΔP_{RG} is considered 5%, representing the pressure drop and the regenerator (Valero et al. 1994)
Combustion chamber	$\dot{m}_a h_3 + \dot{m}_f LHV_f = \dot{m}_g h_4 + (1 - \eta_{CC}) \dot{m}_f LHV_f$ $\frac{P_6}{P_5} = (1 - \Delta P_{CC})$	$\dot{m}_f, \eta_{CC} = 98\%$, and $\Delta P_{CC} = 5\%$ are fuel mass flow rate, efficiency, and pressure drop within the combustion chamber, respectively (Valero et al. 1994)
High-pressure gas turbine	$T_7 = T_6 \left(1 - \eta_{GT} \left(1 - \left(\frac{P_6}{P_7} \right)^{\frac{1-\gamma_g}{\gamma_g}} \right) \right)$ $\dot{W}_{GT-H} = \dot{m}_g \int_{T_6}^{T_7} C_{p_g} dT$ $C_{p_g}(T) = 0.991 \left(\frac{6.99T}{10^2} \right) + \left(\frac{2.712T^2}{10^7} \right) - \left(\frac{1.2244T^3}{10^{10}} \right)$	C_{p_g} is the specific heat a constant pressure of flue gas, which is given as a function of temperature (Ahmadi et al. 2011; Valero et al. 1994)
Low-pressure gas turbine	$T_9 = T_8 \left(1 - \eta_{GT} \left(1 - \left(\frac{P_8}{P_9} \right)^{\frac{1-\gamma_g}{\gamma_g}} \right) \right)$ $\dot{W}_{GT-L} = \dot{m}_g \int_{T_8}^{T_9} C_{p_g} dT$ $C_{p_g}(T) = 0.991 \left(\frac{6.99T}{10^2} \right) + \left(\frac{2.712T^2}{10^7} \right) - \left(\frac{1.2244T^3}{10^{10}} \right)$	Ahmadi et al. (2011), Valero et al. (1994)

Table 2 The required equations for modeling the air intercooler unit (Kays and London 1984)

Term	Description	Correlation
General pressure drop equation	ΔP is heat exchanger core pressure drop, K_c and K_e are respectively defined as entrance and exit loss coefficients, G introduces minimum free-flow area, f is a flow-friction factor, σ is calculated as a ratio of free-flow to the frontal area of one side of the exchanger	$\frac{\Delta P}{P_1} = \frac{G^2 v_1}{2g_c P_1} \left[\underbrace{\left(K_c + 1 - \sigma^2 \right)}_{\text{Entrance effect}} + 2 \underbrace{\left(\frac{v_2}{v_1} - 1 \right)}_{\text{Flow acceleration}} + \underbrace{f \frac{A}{A_c} \frac{v_m}{v_1}}_{\text{Core friction}} - \underbrace{(1 - \sigma^2 - K_e) \frac{v_2}{v_1}}_{\text{Exit effect}} \right]$
Pressure drops through matrix surfaces or normally flows to the tube	In these types of heat exchangers, the entrance and exit coefficients are assumed to be negligible ($K_c, K_e=0$), A is considered as the total transfer area of one side of the exchanger, A_c is the free-flow area of one side, T_{av} and P_{av} are arithmetic averages of the terminal magnitudes, T_{lma} is related to the logarithmic-mean temperature difference between the fluids NOTE: The porosity ρ replaces σ for matrix surfaces	$\frac{\Delta P}{P_1} = \frac{G^2 v_1}{2g_c P_1} \left[\underbrace{(1 + \sigma^2) \left(\frac{v_2}{v_1} - 1 \right)}_{\text{Flow acceleration}} + \underbrace{f \frac{A}{A_c} \frac{v_m}{v_1}}_{\text{Core friction}} \right]$ $\frac{A}{A_c} = \frac{L}{r_h}$ $\frac{G^2 v_1}{2g_c P_1} = \frac{(V_1^2/2g_c)}{(P_1/\rho_1)}$ $v_m = \frac{1}{A} \int_0^A v dA$ $\frac{v_m}{v_1} \approx \frac{P_1 T_{av}}{P_{av} T_1} \Rightarrow \frac{v_m}{v_1} \approx \frac{P_1 T_{lma}}{P_{av} T_1}$ $T_{lma} = T_{const} \pm \Delta t_{lma}$ $\Delta t_{lma} = \frac{(t_{h,in}-t_c)-(t_{h,out}-t_c)}{\ln[(t_{h,in}-t_c)/(t_{h,out}-t_c)]} = \frac{t_{h,in}-t_{h,out}}{N_w}$
Core velocity equation	$(\Delta P/P)$ is the allowable pressure drop on each side, L is the flow length on one side, and r_h is defined as the flow passage hydraulic radius	$\frac{V_1^2/2g_c}{P_1/\rho_1} \approx \left(\frac{\Delta P/P}{N_w} \right)_{\text{oneside}} \frac{\rho_w N_{St}}{\rho_1 f} \eta_0$ $(N_w)_{\text{oneside}} = \left(\eta \frac{L}{r_h} N_{St} \right)_{\text{oneside}}$

3.1.1 The Modified RBC

The BC is the main power generator in the combined power cycle and plays a significant role in generating power and heat. The wasted heat in the BC can generate high-pressure steam in the RC. The ERC also uses the wasted heat to produce a cooling load. To increase the efficiency of the BC, air compression and expansion are done by double-stage compressors and turbines with intermediate cooling and heating. The equations required to model this subsystem are presented in Table 1.

As noted before, the air intercooler unit is used in configuration No. 1. Unlike most previous research that modeled the air intercooler by simplifying assumptions, the thermodynamics and fluid flow principles are utilized in this study to develop an accurate model that considers the physical phenomenon inside it. The required equations are summarized in Table 2, and the T-s diagram of the cycle is depicted in Fig. 3.

3.1.2 The RC

The RC is one of the most critical power generation systems combined with the BC to form a united power cycle. This

system is connected to the BC by HRSG. The output of the gas turbine enters the HRSG, and high-pressure steam is generated and then sent to the steam turbine. By applying ΔP_{inch} , defined as the temperature difference between the saturation state and the evaporator output gas, the temperature parameters of output gas can be obtained throughout the dual-pressure HRSG. Moreover, the approach refers to the temperature differences between the saturation state and economizer outlet water.

The modeling of the RC is presented in Table 3, and its T-s is depicted in Fig. 4.

3.1.3 The ERC

The ERC operates with heat input energy. This system includes an ejector, generator, evaporator, condenser, pump, and expansion valve. The main component of this system is the ejector, which comprises four sub-components, including the primary nozzle, mixing chamber, throat, and diffuser, which acts as a compressor in this system and replaces it. In other words, the ejector converts the mechanical energy of the working fluid to kinetic energy without any rotating equipment. Hence, it is known as an economic refrigeration cycle with acceptable efficiency and, therefore, can

Table 3 Energy balance equations for components of the RC (Cengel and Boles 2006)

Component	Energy balance	
	System 1	System 2
Economizer	$\dot{m}_{st}(h_{14} - h_{13}) = \dot{m}_g \int_{T_D}^{T_C} C_{P_g} dT$	$\dot{m}_{st}(h_{15} - h_{14}) = \dot{m}_g \int_{T_D}^{T_C} C_{P_g} dT$
Evaporator	$\dot{m}_{st}(h_{15} - h_{14}) = \dot{m}_g \int_{T_C}^{T_B} C_{P_g} dT$	$\dot{m}_{st}(h_{16} - h_{15}) = \dot{m}_g \int_{T_C}^{T_B} C_{P_g} dT$
Superheater	$\dot{m}_{st}(h_{16} - h_{15}) = \dot{m}_g \int_{T_B}^{T_A} C_{P_g} dT$	$\dot{m}_{st}(h_{17} - h_{16}) = \dot{m}_g \int_{T_B}^{T_A} C_{P_g} dT$
Steam turbine	$\dot{W}_{ST} = \dot{m}_{st}(h_{16} - h_{17}), \eta_{ST} = \frac{\dot{W}_{ST,actual}}{\dot{W}_{ST,is}}$	$\dot{W}_{ST} = \dot{m}_{st}(h_{17} - h_{18}), \eta_{ST} = \frac{\dot{W}_{ST,actual}}{\dot{W}_{ST,is}}$
Steam condenser	$\dot{Q}_{cond} = \dot{m}_{st}(h_{17} - h_{12})$	$\dot{Q}_{cond} = \dot{m}_{st}(h_{18} - h_{13})$
Feed water pump	$\dot{W}_{FWP} = \dot{m}_{st}(h_{12} - h_{13}), \eta_{FWP} = \frac{\dot{W}_{FWP,is}}{\dot{W}_{FWP,actual}}$	$\dot{W}_{FWP} = \dot{m}_{st}(h_{13} - h_{14}), \eta_{FWP} = \frac{\dot{W}_{FWP,is}}{\dot{W}_{FWP,actual}}$

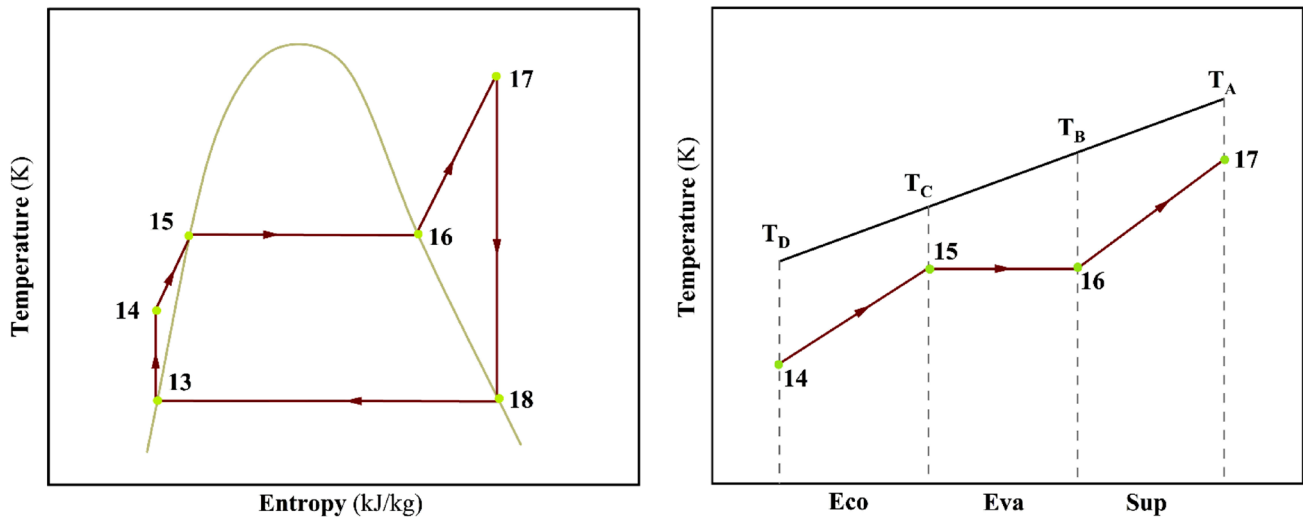


Fig. 4 T-s diagram of the Rankine cycle and temperature profile within the HRSG

be an excellent alternative to the ARC. The modeling of this system is presented in Table 4. It should be noted that the ejector is modeled by trial and error to obtain the final value of the mass entrainment ratio (μ). In the process of modeling this system, the following assumptions have been considered:

- The heat transfer rate between the ejector and the surroundings can be eliminated. The velocity change for the streams in the inlet and outlet ports of the ERC components is assumed to be negligible except for the ejector.
- Effects of the mixing section, nozzle, and frictional and mixing losses in the diffuser are modeled by applying the nozzle, diffuser, and mixing efficiencies.
- Upstream of the diffuser inlet is considered as the place where normal shock wave often happens.
- Constant pressure mode is considered for the mixing process in the ejector.

Regarding the mentioned assumptions, the energy, momentum, and mass equations for each part of the ejector are reported in Table 4 (Dai et al. 2009). Also, the related T-s diagram is depicted in Fig. 5.

3.2 Exergy Analysis

Various strategies have been developed in thermal analyses to examine the performance of energy systems, including exergy and energy analyses. Many researchers have pointed out that results from exergy analysis are more practical for systems appraisal since they can provide engineers with feasible approaches to harness the available energy efficiently. Moreover, the exergy assessment can detect destructions' exact locations and magnitude. In cases where potential and kinetic exergy can be assumed to be negligible, exergy will consist of two major parts: physical and chemical exergies.

Table 4 Energy balance equations for components of the ERC (Dai et al. 2009)

Different sub-components of the ejector should be modeled due to the complexity of the physical phenomenon (i.e., severe pressure and velocity changes) inside it:

Primary nozzle (PN):

Energy conservation equation:

$$h_{PF,o} + \frac{v_{PF,o}^2}{2} = h_{PF,i} + \frac{v_{PF,i}^2}{2}$$

Enthalpy of flow at the primary nozzle exit (η_{PN} , the primary nozzle efficiency):

$$h_{PF,o} = h_{PF,i}(1 - \eta_{PN}) + \eta_{PN}h_{PF,o, is}$$

The inlet's primary flow velocity, $v_{PF,ni}$ is negligible compared to the outlet's primary flow velocity, $v_{PF,ne}$. The outlet velocity of the primary flow $v_{PF,o}$ is:

$$v_{PF,o} = \sqrt{2\eta_{PN}(h_{PF,i} - h_{PF,o, is})}$$

The same relation is derived for secondary flow:

$$v_{SF,o} = \sqrt{2(h_{SF,ni} - h_{SF,ne})}$$

The ejector entrainment ratio is:

$$\mu = \frac{\dot{m}_{SF}}{\dot{m}_{PF}}$$

Mixing chamber (MC):

The mixing section velocity obtained from the momentum conservation equation:

$$v_{MF} = \sqrt{\eta_{MC} \left(\frac{v_{PF,o} + \mu v_{SF,o}}{1 + \mu} \right)^2}$$

Mixing efficiency is:

$$\eta_{MC} = \frac{v_{MF}^2}{v_{MF, is}^2}$$

Energy conservation equation for mixing section:

$$\dot{m}_{PF} \left(h_{PF,o} + \frac{v_{PF,o}^2}{2} \right) + \dot{m}_{SF} \left(h_{SF,o} + \frac{v_{SF,o}^2}{2} \right) = (\dot{m}_{PF} + \dot{m}_{SF}) \left(h_{MF} + \frac{v_{MF}^2}{2} \right)$$

Enthalpy of the mixed flow:

$$h_{MF} = \frac{h_{PF,i} + \mu h_{SF,i}}{1 + \mu} - \frac{v_{MF}^2}{2}$$

Diffuser (D):

The energy equation for the diffuser:

$$\frac{v_{MF}^2 - v_D^2}{2} = h_D - h_{MF}$$

Enthalpy of flow at the ejector exit:

$$h_D = h_{MF} + v_D^2/2$$

Actual flow enthalpy at diffuser exit (η_d , the diffuser efficiency):

$$h_D = \frac{h_{D, is} - h_{MF}}{\eta_d} + h_{MF}$$

Entrainment ratio:

$$\mu = \sqrt{\eta_{PN}\eta_{MC}\eta_D(h_{PF,i} - h_{PF,o, is}) / (h_{D, is} - h_{MF})} - 1$$

The refrigeration cycle components are modeled by applying the energy conservation law. The obtained equations can be shown in the following:

For generator:

$$\dot{Q}_{gen} = \dot{m}_{PF}(h_{19} - h_{24})$$

For ERC condenser:

$$\dot{Q}_{cond} = (\dot{m}_{PF} + \dot{m}_{SF})(h_{20} - h_{21})$$

For intercooler:

$$\dot{Q}_{int} = \dot{m}_{SF}(h_{25} - h_{26})$$

For pump:

$$\dot{W}_{pump} = \dot{m}_{PF}(h_{24} - h_{22})$$

The second law of thermodynamics provides the exergy destruction rate, which can be expressed as follows Dincer and Rosen (2007):

$$\dot{E}x_Q + \left(\sum \dot{m}_{in} ex_{in} \right) = \left(\sum \dot{m}_{out} ex_{out} \right) + \dot{E}x_W + \dot{E}x_{des} \quad (3)$$

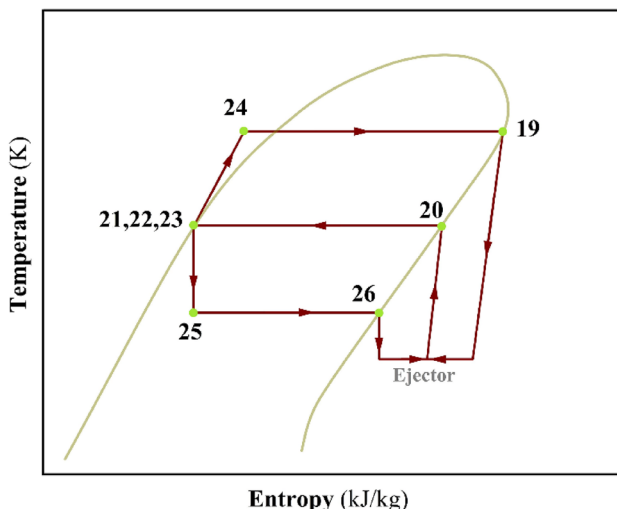


Fig. 5 T-s diagram of the ejector refrigeration cycle

$$ex = ex_{ph} + ex_{ch} \tag{4}$$

where the equation related to the exergy transfer via heat ($\dot{E}x_Q$) and work ($\dot{E}x_W$) can be written as Eqs. (5) and (6). Also, the chemical and physical exergy terms are expressed in Eq. (7) (Bejan et al. 1996).

$$\dot{E}x_Q = \left(1 - \frac{T_0}{T_i}\right) \dot{Q}_i \tag{5}$$

$$\dot{E}x_W = \dot{W} \tag{6}$$

$$ex_{ch,mix} = \sum_i^n X_i ex_{ch_i} + RT_0 \sum_{i=1}^n X_i \ln(X_i)$$

$$ex_{ph} = \dot{m}((h - h_0) - T_0(s - s_0)) \tag{7}$$

where the subscript (0) stands for the ambient conditions.

Table 5 reports the exergy destruction rate in terms of the different components of the proposed CCHP system.

3.3 Economic Analysis

When proposing new systems, it should be noted that a system with better efficiency is not always the best answer. One of the most important factors in the success of a new system is its ability to compete economically with other systems. As a result, economic analysis should always be considered alongside thermodynamic analysis. Economic analysis includes the initial purchase price of equipment, maintenance costs, and fuel costs. The total annual cost rate is determined as follows (Bejan et al. 1996; Mahmoudan et al. 2022):

Table 5 Expressions for exergy destruction rate within components (Cengel and Boles 2006)

Component	Exergy destruction rate	
	System 1	System 2
Air compressor 1	$\dot{E}x_{des,AC_1} = \dot{E}x_1 - \dot{E}x_2 + \dot{W}_{AC_1}$	$\dot{E}x_{des,AC_1} = \dot{E}x_1 - \dot{E}x_2 + \dot{W}_{AC_1}$
Air intercooler	$\dot{E}x_{des,int} = \dot{E}x_2 - \dot{E}x_3 - \dot{E}x_{Q_{int}}$	$\dot{E}x_{des,int} = \dot{E}x_2 + \dot{E}x_{25} - \dot{E}x_3 - \dot{E}x_{26}$
Air compressor 2	$\dot{E}x_{des,AC_2} = \dot{E}x_3 - \dot{E}x_4 + \dot{W}_{AC_2}$	$\dot{E}x_{des,AC_2} = \dot{E}x_3 - \dot{E}x_4 + \dot{W}_{AC_2}$
Regenerator	$\dot{E}x_{des,RG} = \dot{E}x_4 + \dot{E}x_9 - \dot{E}x_5 - \dot{E}x_{10}$	$\dot{E}x_{des,RG} = \dot{E}x_4 + \dot{E}x_9 - \dot{E}x_5 - \dot{E}x_{10}$
Combustion chamber	$\dot{E}x_{des,CC} = \dot{E}x_5 + \dot{E}x_f - \dot{E}x_6$	$\dot{E}x_{des,CC} = \dot{E}x_5 + \dot{E}x_f - \dot{E}x_6$
High-pressure gas turbine	$\dot{E}x_{des,GT_1} = \dot{E}x_6 - \dot{E}x_7 - \dot{W}_{GT_1}$	$\dot{E}x_{des,GT_1} = \dot{E}x_6 - \dot{E}x_7 - \dot{W}_{GT_1}$
Reheater	$\dot{E}x_{des,RH} = \dot{E}x_7 - \dot{E}x_8 - \dot{E}x_{Q_{RH}}$	$\dot{E}x_{des,RH} = \dot{E}x_7 - \dot{E}x_8 - \dot{E}x_{Q_{RH}}$
Low-pressure gas turbine	$\dot{E}x_{des,GT_2} = \dot{E}x_8 - \dot{E}x_9 - \dot{W}_{GT_2}$	$\dot{E}x_{des,GT_2} = \dot{E}x_8 - \dot{E}x_9 - \dot{W}_{GT_2}$
HRSG	$\dot{E}x_{des,HRSG} = \dot{E}x_{10} + \dot{E}x_{13} - \dot{E}x_{11} - \dot{E}x_{16}$	$\dot{E}x_{des,HRSG} = \dot{E}x_{10} + \dot{E}x_{14} - \dot{E}x_{11} - \dot{E}x_{17}$
Steam turbine	$\dot{E}x_{des,ST} = \dot{E}x_{16} - \dot{E}x_{17} - \dot{W}_{ST}$	$\dot{E}x_{des,ST} = \dot{E}x_{17} - \dot{E}x_{18} - \dot{W}_{ST}$
Steam condenser	$\dot{E}x_{des,cond} = \dot{E}x_{17} - \dot{E}x_{12} - \dot{E}x_{Q_{cond}}$	$\dot{E}x_{des,cond_1} = \dot{E}x_{18} - \dot{E}x_{13} - \dot{E}x_{Q_{cond_1}}$
Feed water pump	$\dot{E}x_{des,FWP} = \dot{E}x_{12} - \dot{E}x_{13} + \dot{W}_{FWP}$	$\dot{E}x_{des,FWP} = \dot{E}x_{13} - \dot{E}x_{14} + \dot{W}_{FWP}$
ERC ejector	-	$\dot{E}x_{des,ejector} = \dot{E}x_{19} + \dot{E}x_{26} - \dot{E}x_{20}$
ERC generator	-	$\dot{E}x_{des,gen} = \dot{E}x_{11} + \dot{E}x_{24} - \dot{E}x_{12} - \dot{E}x_{19}$
ERC condenser	-	$\dot{E}x_{des,cond_2} = \dot{E}x_{20} - \dot{E}x_{21} - \dot{E}x_{Q_{cond_2}}$
ERC pump	-	$\dot{E}x_{des,pump} = \dot{E}x_{22} - \dot{E}x_{24} + \dot{W}_{pump}$
ERC expansion valve	-	$\dot{E}x_{des,EV} = \dot{E}x_{23} - \dot{E}x_{25}$

Table 6 Capital cost of components (Ebrahimi-Moghadam and Farzaneh-Gord 2021; Wang et al. 2022a)

Component	Cost functions (\$)
Air compressors 1	$Z_{AC,1} = \left(\frac{39.5\dot{m}_a}{0.9-\eta_{AC}}\right)\left(\frac{P_2}{P_1}\right) \times \ln\left(\frac{P_2}{P_1}\right)$
Air compressors 2	$Z_{AC,2} = \left(\frac{39.5\dot{m}_a}{0.9-\eta_{AC}}\right)\left(\frac{P_4}{P_3}\right) \times \ln\left(\frac{P_4}{P_3}\right)$
Combustion chamber	$Z_{CC} = \left(\frac{25.6\dot{m}_a}{0.995-\frac{P_8}{P_5}}\right)[1 + \exp(0.018T_6 - 26.4)]$
High-pressure gas turbine	$Z_{GT,1} = \left(\frac{266.3\dot{m}_g}{0.92-\eta_{GT}}\right) \times \ln\left(\frac{P_6}{P_7}\right)[1 + \exp(0.036T_6 - 54.4)]$
Low-pressure gas turbine	$Z_{GT,2} = \left(\frac{266.3\dot{m}_g}{0.92-\eta_{GT}}\right) \times \ln\left(\frac{P_8}{P_9}\right)[1 + \exp(0.036T_8 - 54.4)]$
Regenerator	$Z_{RG} = 2290\left(\frac{\dot{m}_g(h_9-h_{10})}{U(\Delta T_{LMTD})}\right)^{0.6}$
Electric generator	$Z_{gen} = 60E_P^{0.95}$
Steam turbine	$Z_{ST} = 3880.5 \times \dot{W}_{ST}^{0.7} \times \left(1 + \left(\frac{0.05}{1-\eta_{ST}}\right)^3\right) \times \left(1 + 5 \times \exp\left(\frac{T_m-866}{10.42}\right)\right)$
Pumps	$Z_{pump} = 705.48 \times \dot{W}_{pump}^{0.71} \left(1 + \frac{0.2}{1-\eta_{pump}}\right)$
Condensers	$Z_{cond} = 1773\dot{m}_s$
Heat exchangers	$Z_{HE} = 130(A_{HE}/0.093)^{0.78}$
Ejector	$Z_{ejector} = 1000 \times 16.14 \times 0.989 \times (\dot{m}_{19}(T_{19}/P_{19}^{0.05})P_{20}^{-0.75})$

$$\dot{C}_{tot} = \dot{C}_f + \sum_k \dot{Z}_k \tag{8}$$

$$\dot{C}_f = (C_f \dot{m}_f LHV_f) \times t \tag{9}$$

$$\dot{Z} = CRF \times Z \times \varphi \tag{10}$$

where \dot{Z}_k is the rate of investment (Z) and the maintenance costs for the k th component. Also, \dot{C}_f , t , and φ are fuel cost, the number of working hours, and maintenance factor (1.06 in this study) (Alirahmi et al. 2020), respectively. Table 6 shows the cost equation for each component of the system.

The capital recovery factor (CRF) calculates the leveled cost. The CRF is expressed as follows Tozlu et al. (2021):

$$CRF = i_{eff} \frac{(1 + i_{eff})^N}{(1 + i_{eff})^N - 1} \tag{11}$$

where N and i_{eff} describe the system lifetime (25 years in this study) and effective annual interest rate (10% in this study Karimi et al. 2020). The costs are updated by using the Chemical Engineering Plant Cost Index (CEPCI) (<https://www.chemengonline.com/>):

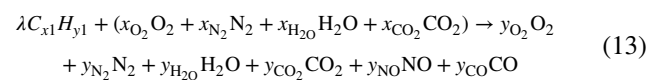
$$\dot{Z}_{2020} = \dot{Z} \frac{CI_{present}}{CI_{reference}} \tag{12}$$

where $CI_{present}$ presents the year cost index, and $CI_{reference}$ is the reference year cost index.

3.4 Environmental Analysis

The impact of the introduced power plant on the environment is also assessed in this investigation. As the most important pollutant of the BC, the released carbon dioxide (CO₂) into the atmosphere per system production is presented to evaluate the environmental condition of the system. Unlike most previous studies, which considered a constant value of CO₂ per amount of generated power, the released CO₂ in this study is determined based on the combustion reaction.

Generally, the chemical formulation of the combustion reaction for any hydrocarbon (C_{x1}H_{y1}) is written as follows Ahmadi and Dincer (2010):



For calculating the amount of the released pollutants, this reaction should be solved by applying the molar balances as follows:

$$\text{Carbon balance : } y_{CO_2} = \bar{\lambda}x_1 + x_{CO_2} - y_{CO}$$

$$\text{Hydrogen balance : } y_{H_2O} = x_{H_2O} + \frac{\bar{\lambda}x_2}{2}$$

$$\text{Oxygen balance : } y_{O_2} = x_{O_2} - \bar{\lambda}x_1 - \frac{\bar{\lambda}x_2}{4} - \frac{y_{NO}}{2} - \frac{y_{CO}}{2}$$

$$\text{Nitrogen balance : } y_{N_2} = x_{N_2} - y_{NO} \tag{14}$$

3.5 Performance Criteria

To evaluate the performance of the proposed system from 4E points of view, the energy and exergy efficiencies, levelized carbon dioxide emission, and levelized cost of electricity generation are defined as follows Cengel and Boles (2006):

$$\text{Energy efficiency} = \eta_{th} = \frac{\dot{W}_{net,GT} + \dot{W}_{ST}}{\dot{m}_f \times \text{LHV}_f} \quad (15)$$

$$\text{Exergy efficiency} = \eta_{ex} = \frac{\dot{W}_{net,GT} + \dot{W}_{ST}}{\dot{E}x_f} \quad (16)$$

$$\text{Levelized CO}_2 \text{ emission} = \zeta_{CO_2} = \frac{\dot{m}_{CO_2}}{\dot{W}_{net}} \quad (17)$$

$$\text{Levelized cost of electricity} = \text{LCOE} = \frac{\dot{C}_{tot}}{\dot{W}_{net}} \quad (18)$$

3.6 Problem Solution and Optimization Procedures

The present model is computationally coded in the MATLAB software package. Since the thermodynamic properties of the working fluids in different states of the system are required, REFPROP 9.0 (Lemmon et al. 2010) is linked up with MATLAB. As a parametric sensitivity analysis, the

effects of five key design parameters are evaluated on the system performance. Based on the considered value of the simulation input data (presented in Table 7), the appropriate range of these five parameters is selected for thermodynamically optimal system operation.

It is worth mentioning that the mass flow rates of the working fluids in all cycles are not considered to be fixed as the problem input parameters. In other words, the governing equations are solved based on the “variable system sizing” process. It means that depending on the considered value of the design and input parameters, the corresponding value of the working fluids' mass flow rates is calculated using the trial and error approach. It is while that most of the previously published works in the field of study considered a fixed system size in their analyses for simplification.

Finally, as a genetic-based optimization approach, a multi-objective NSGA-II optimization method is applied to reach the optimal value of the objective functions (Gu et al. 2023; Wang et al. 2022b). The NSGA-II is based on an evolutionary algorithm widely used in literature, as it gives reliable answers in energy systems optimization. This method contains different steps (shown in Fig. 6) and requires some assumptions, and their appropriate values should be selected based on the problem under investigation (presented in Table 7).

It should be noted that the power generation of the combined cycle is fixed at 40 MW. Natural gas is the fuel (with a lower heating value of $\text{LHV}_f = 50,000 \text{ kJ/kg}$). Furthermore,

Table 7 Simulation input data of the CCHP cycle (Ahmadi et al. 2011; Hosseini et al. 2013)

	Term	Value	Term	Value
Modeling input data	Ambient temperature	25 °C	ERC condenser temperature	30 °C
	Ambient pressure	1.01 bar	ERC generator temperature	95 °C
	Inlet air molar contents	0.7748 N ₂ , 0.2059 O ₂ , 0.019 H ₂ O, and 0.0003 CO ₂	Regenerator effectiveness	81%
	Compressor pressure ratio	8.52	Combustion chamber efficiency	98%
	Gas turbine inlet temperature	1220 °C	Isentropic efficiency of AC compressor	85%
	Steam pressure	50 bar	Isentropic efficiency of GT turbine	88%
	Steam condensation pressure	0.1 bar	HRSG pinch point temperature difference	50 °C
	ERC evaporator temperature	5 °C	HRSG approach point temperature difference	10 °C
Design parameters	Compressor pressure ratio	$2 \leq \text{PR} \leq 16$	Steam pressure	$20 \text{ bar} \leq P_{st} \leq 80 \text{ bar}$
	Gas turbine inlet temperature	$1200 \text{ K} \leq T_{GT} \leq 1600 \text{ K}$	Steam turbine inlet temperature	$600 \text{ °C} \leq T_{ST} \leq 700 \text{ °C}$
	Pinch point temperature difference	$10 \text{ K} \leq \Delta T_{pp} \leq 80 \text{ K}$		
Optimization assumptions	Individuals number of the population	50	Mutation probability	0.3
	Generations number	110	Crossover probability	0.8

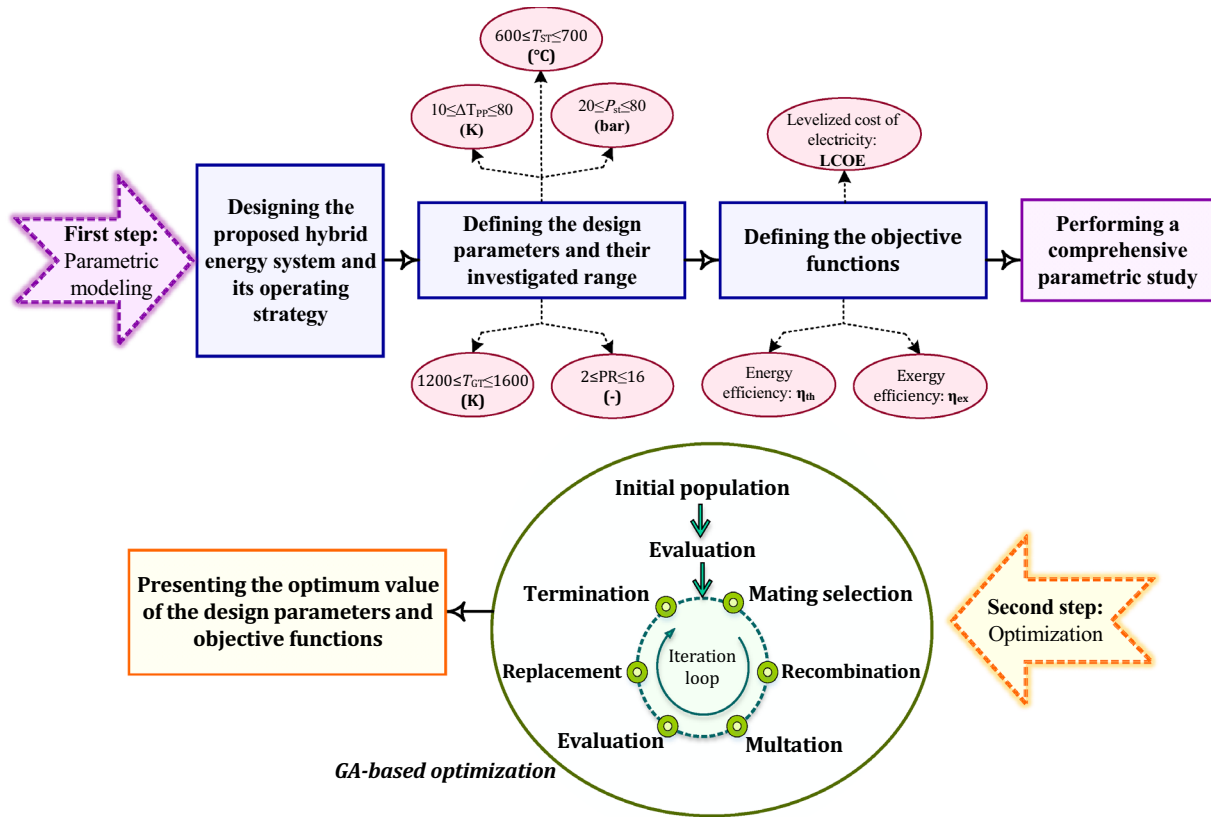


Fig. 6 Schematic flowchart of the problem solution and optimization procedures

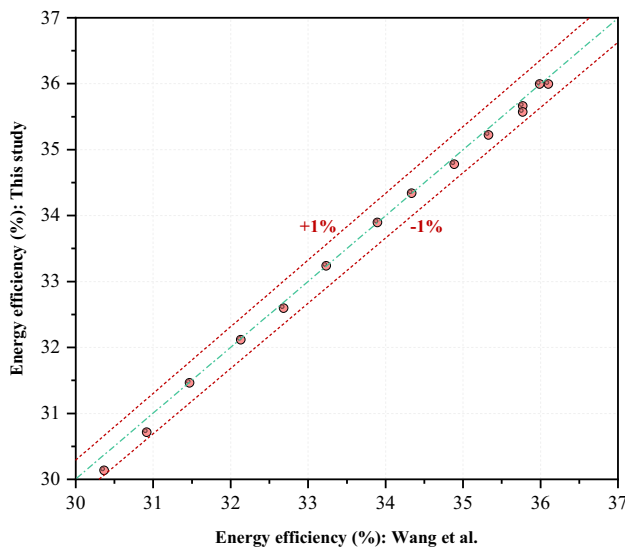


Fig. 7 Validation of the regenerative Brayton cycle modeling results (Ebrahimi-Moghadam and Farzaneh-Gord 2021)

R141b is ERC working fluid. Table 7 presents the input parameters.

Table 8 Validation of the ejector refrigeration cycle modeling results (Wang et al. 2022a)

Primary flow temperature (°C)	Ejector's entrainment ratio (μ)		Relative error percentage
	Reference study	This study	
78	0.287	0.275	4.18
84	0.263	0.251	4.56
90	0.237	0.224	5.49
95	0.197	0.189	4.06

4 Validation

To prove the correctness of the problem–solution procedure, component validation is necessary. For this, the results of the developed computational code in this study are compared with the results obtained by Ebrahimi-Moghadam and Farzaneh-Gord (2021) (Fig. 7) and Wang et al. (2022a) (Table 8) for the RBC and ERC, respectively. For the RBC, the compressor pressure ratio was varied between 5 and 20 (by an interval of 1), and comparing the results showed that the maximum and minimum relative deviations are 0.77% and 0.0009%. Also, the ERC's maximum and minimum

Table 9 The main results of energetic and exergetic analyses (RBC: regenerative BC, Reh: with reheater, Int: with intercooler)

System	Fuel rate (kg/s)	Energy efficiency (%)	Exergy efficiency (%)
BC	2.539	31.53	30.18
RBC	1.782	44.92	43.00
RBC-Reh	1.682	47.59	45.55
RBC-Int (compact HX)-Reh	1.616	49.56	47.44
RBC-Int (ERC)-Reh	1.656	48.36	46.30
RBC-ST	1.489	53.74	51.44
RBC-Int (compact HX)-Reh-ST	1.493	53.65	51.36
RBC-Int (ERC)-Reh-ST	1.433	55.84	53.46

relative deviations are obtained as 5.49% and 4.06%, respectively. It reveals the excellent match between the results, and the reason for higher deviations for the ERC is due to the complexity of the ejector's energetic model.

5 Results and Discussion

This section focuses on three goals: Firstly, a comparative technical analysis compares the efficiency of different system configurations and demonstrates the reason for choosing the proposed layouts and their superiority over other possible structures. Afterward, the impact of changing the five design parameters in their range (constantly changing the other parameters) on the defined 4E functions is evaluated. Finally, the optimal value of the system indices is found through a multi-objective optimization approach.

5.1 Comparative Study

To show the superiority of the proposed system in this study, the efficiencies of different types of BCs are compared in Table 9. As mentioned in this research, in addition to providing a hybrid energy system, a modified gas turbine cycle will be used as the mover (aiming to achieve a more efficient system) instead of a base gas turbine mover cycle. Hence, different layouts of intercooling and reheating processes are introduced and compared to select the best one. Afterward, the parametric sensitivity analysis and optimization are applied to the most efficient system.

The energy and exergy efficiencies of the simple BC are 31.53% and 30.18%, respectively. By adding a regenerator to the system and recovering the heat output from the gas turbine to preheat the inlet air to the combustion chamber, the energy and exergy efficiencies reached 44.92% and 43.00%, respectively; a significant fuel consumption reduction is also

observed. Adding a reheater also increases efficiencies by 2.5%. The next step is to make the air compression process in two phases. In this case, with the addition of an air-cooled intercooler, the energy and exergy efficiencies reach 49.56% and 47.44%. However, if an ejector refrigeration system is installed instead of an air-cooled intercooler, the efficiencies will be 48.36% and 46.30%, respectively. As a result, the air-cooled intercooler performs better. We can go further and design a combined gas and steam turbine system. This system has efficiencies of 53.74% and 51.44%. It will have exciting results if an intercooler and a reheater are added to this combined system. When an air-cooled intercooler is used, the system achieves energy and exergy efficiencies of 53.65% and 51.36%. While with the ejector refrigeration system, the efficiencies are 55.84% and 53.46%. It is contrary to the above result (without a steam turbine). It is because the flow rate and temperature of the exhaust gas from the system are higher with ejector refrigeration as an intercooler. As a result, although the performance of the BC is poorer due to the higher flow rate and temperature, the system can produce more power through the RC, and the RGT-Int (ERC)-Reh-ST system achieves the best efficiency.

After proving the prominence of the proposed combined cycle compared to the other possible layouts, the next step presents some outputs of the thermodynamic and economic evaluation of the combined cycle. One of the most important results of the thermodynamic analysis is the amount of exergy destruction in each component. Figure 8 shows the contribution of each component to the total exergy destruction. As can be seen, most exergy destruction occurs in BC, which is equivalent to 92% of the total exergy destruction. The remaining 8% of the destroyed exergy is related to the RC. In BC, most exergy destruction occurs in the combustion chamber. The inherent irreversibility of combustion causes it. Next is the regenerator, which is very high due to the heat transfer between the two fluids with a high temperature difference. Gas turbines and compressors account for about 20% of the exergy destruction. In the RC, most exergy destruction occurs in the HRSG due to the high-temperature difference between the hot and cold fluid, followed by the condenser and turbine. In the second cycle, there is also an ejector refrigeration system. About 9.2% of the total exergy destruction occurs in the cooling system. In this system, the most exergy destruction is within the generator. The second component is the ejector. In this component, two different currents are mixed, changing the pressure. Moreover, this irreversible process causes considerable exergy destruction. It should be noted that the exergy degradation in HRSG for the second cycle is much less than in the first cycle. The reason is that heat transfer is done not only to water but also to the fluid of the cooling system, and more heat transfer takes place, and cooling is produced,

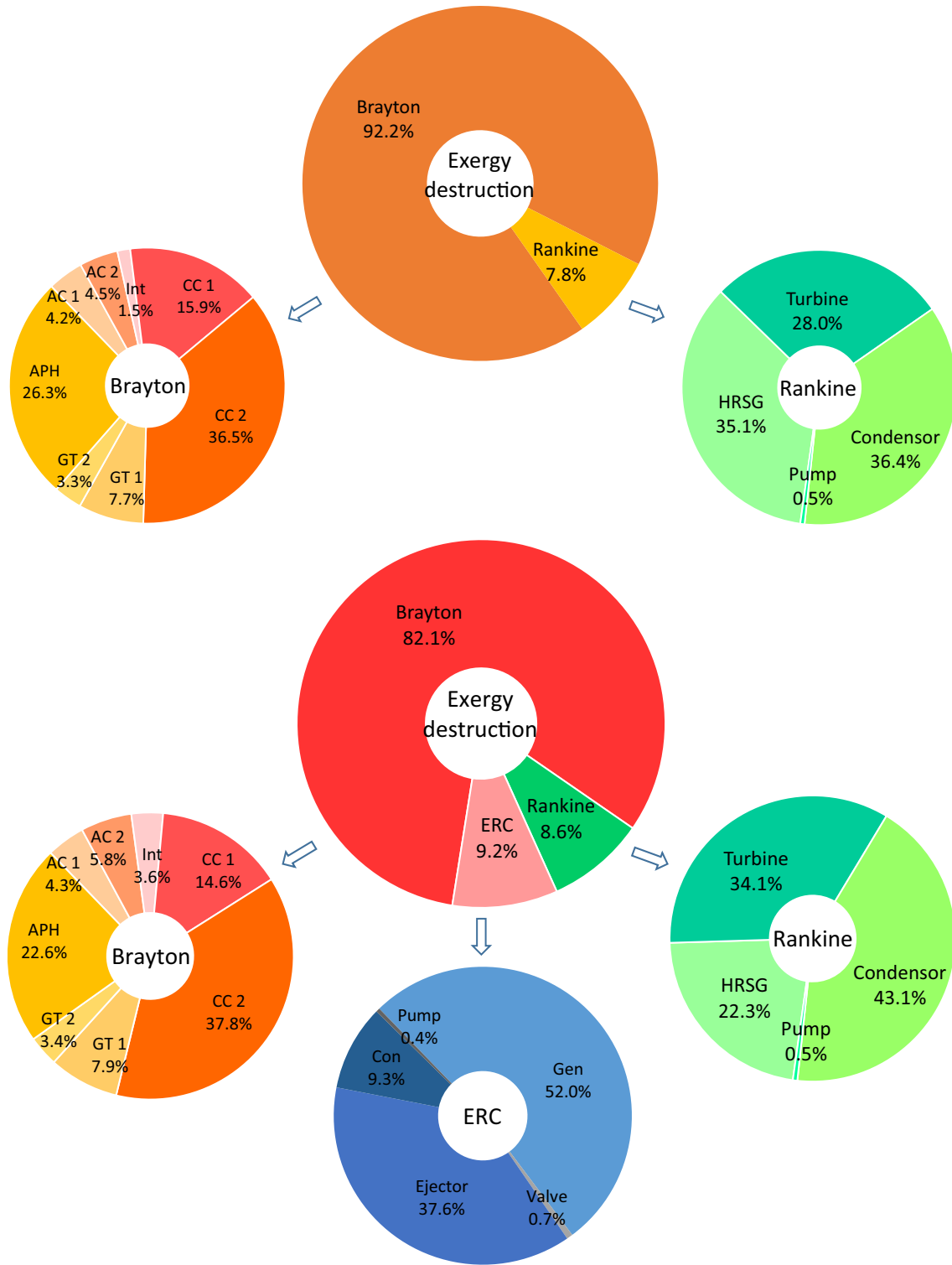


Fig. 8 Contribution of the system components in the exergy destruction

resulting in less exergy destruction. Figure 9 shows how investment costs are distributed among different subsystems and components. Since BC is an upstream system,

it is predictable that it will cost more. In this system, the highest price is related to turbines, and the intercooler is in second place due to its large surface area.

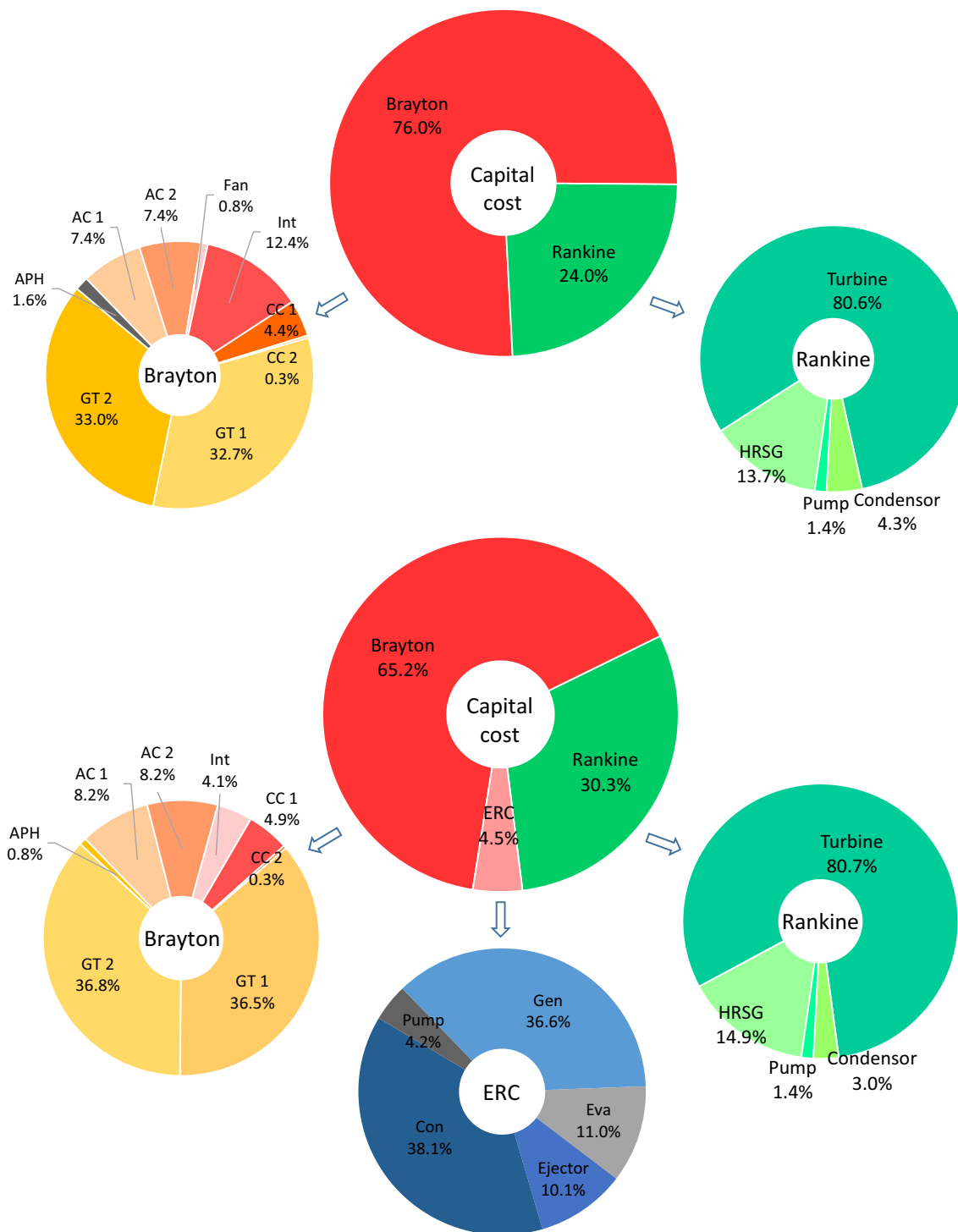


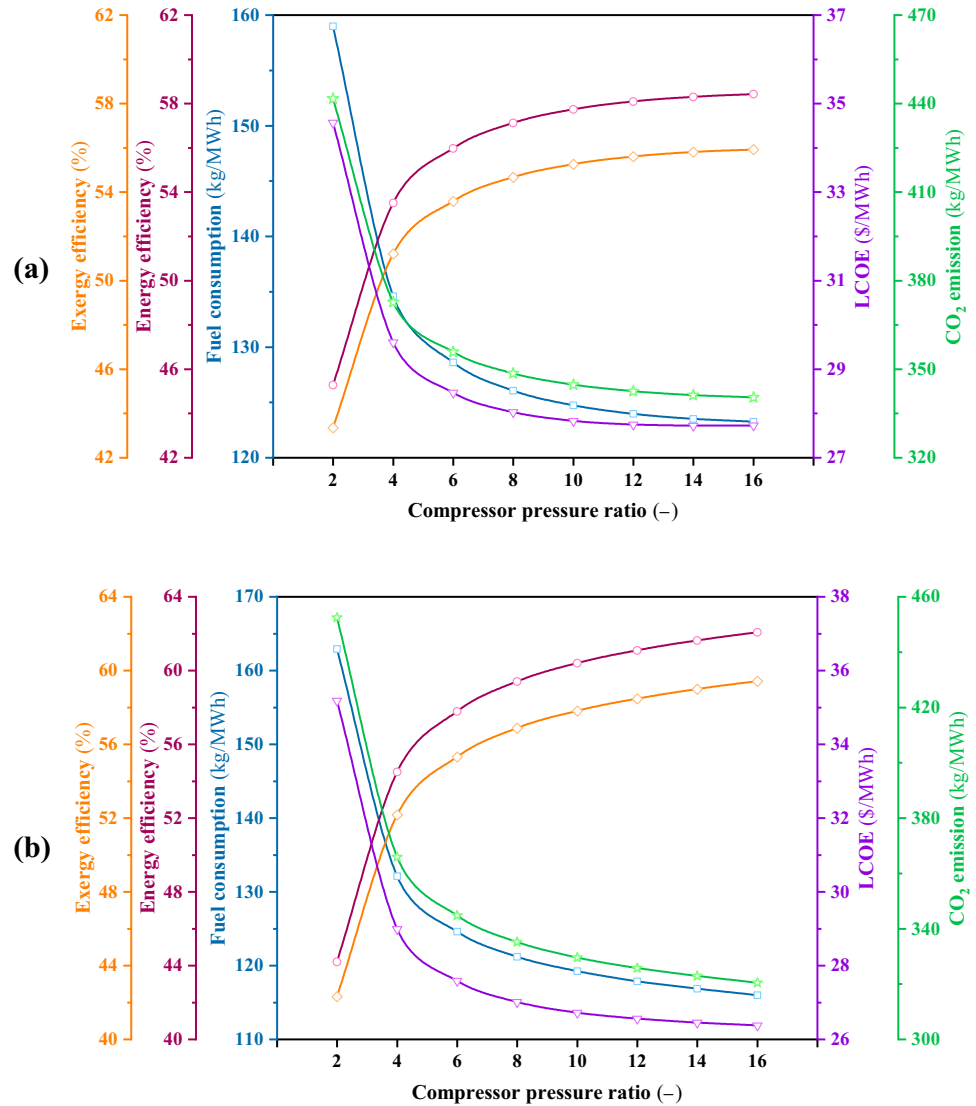
Fig. 9 Contribution of the system components in the capital costs

5.2 Parametric Study

This section examines the effect of different parameters on system performance to obtain a good view of the design parameters. It allows the designer to achieve the best possible efficiency by adjusting the values of the design parameters. It

should be noted that when examining changes in one parameter, the other parameters are kept constant in the values presented in Table 7. In all figures, the values are (1-traditional configuration) for the first integrated system with an air-cooled intercooler and (2-proposed configuration) for the second combined system with an ERC intercooler.

Fig. 10 Effect of compressor pressure ratio on the energetic and exergetic efficiencies, levelized cost of electricity, and levelized CO₂ emission, for the **a** traditional configuration and **b** proposed configuration

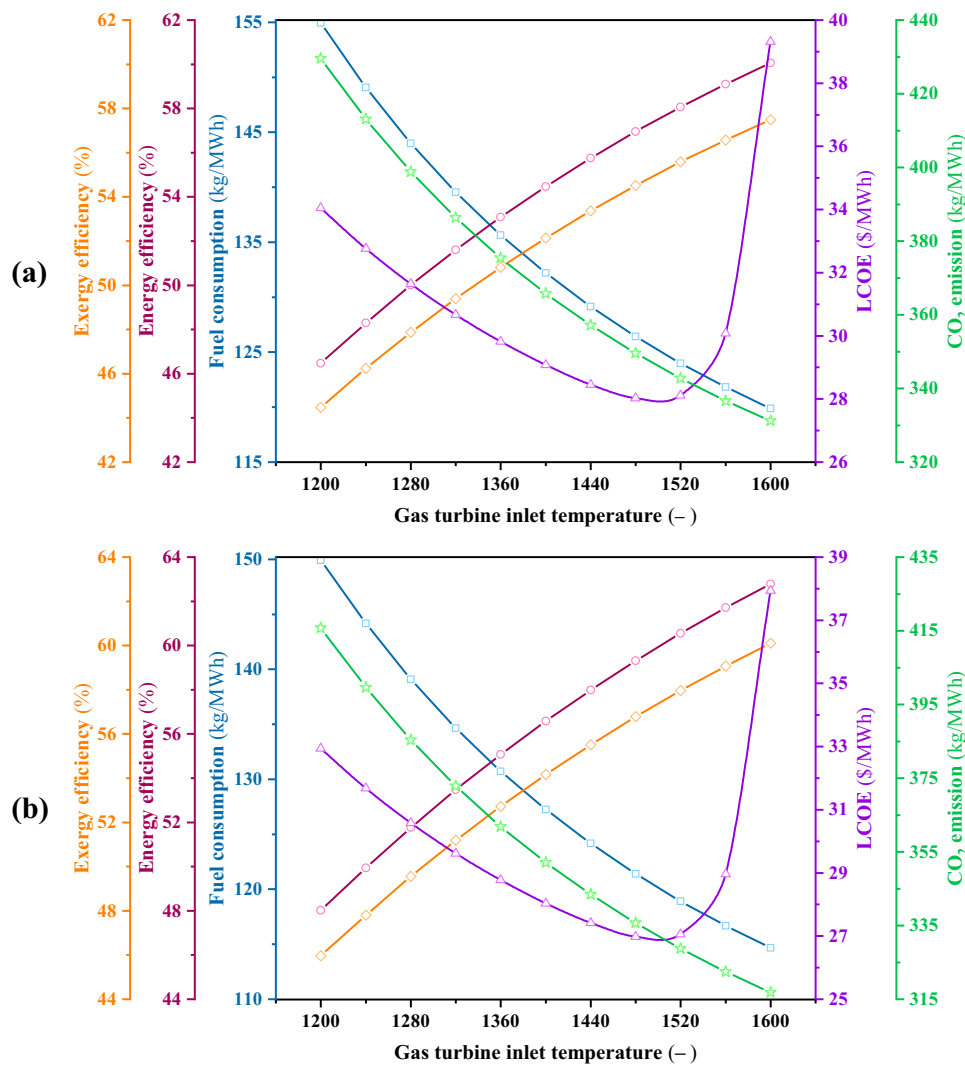


The effect of compressor pressure ratio changes on system performance is shown in Fig. 10. By increasing the pressure ratio from 2 to 16, the fuel consumed decreases because the higher the pressure, the higher the temperature, and vice versa, increasing the pressure or temperature, as mentioned, causes less fuel to compensate for the pressure and temperature. Still, it should be noted that for the pressure ratios between 2 and 4, the change (slope of the chart) is high, and the efficiencies range from about 44% to about 55%. From the pressure ratio of 4 onwards, the slope of the changes becomes less and less so that in values greater than 16, the effect of the changes in the pressure ratio changes is practically negligible. Comparing configurations 2 (proposed) with 1 (traditional) reveals that using the ejector cycle as an intercooler has increased the Brayton-Rankine cycle's thermal and exergy efficiencies. At a PR = 14, the energy efficiency of the traditional configuration is 58.3%, and that of the proposed configuration is 61.62%, concluding that

the proposed configuration has improved the energy efficiency by 5.7%; at a PR = 16, the cycle's exergy efficiency has increased by 6.25%. In the ERC system, since the generator increases the pressure and temperature, the ejector merges this fluid with the cold fluid, bringing the pressure and temperature to a constant level. As a result, it can be said that the pressure difference decreases, and the pump's power consumption decreases. Due to the variable weather conditions, using air coolers somewhat lowers the system's efficiency. However, this temperature is assumed to be constant in cooling exchangers, bringing better heat transfer for the fluid cooler.

Figure 10b also shows the changes in LCOE and emissions. As expected, increasing the pressure ratio reduces carbon dioxide emissions due to reducing fuel consumption. Increasing the ratio from 4 to 8 reduced the system's LCOE from 29 to 27 \$/MWh and CO₂ emission from 366 to 335.2 kg/MWh.

Fig. 11 Effect of gas turbine inlet temperature on the energetic and exergetic efficiencies, levelized cost of electricity, and levelized CO₂ emission, for the **a** traditional configuration and **b** proposed configuration



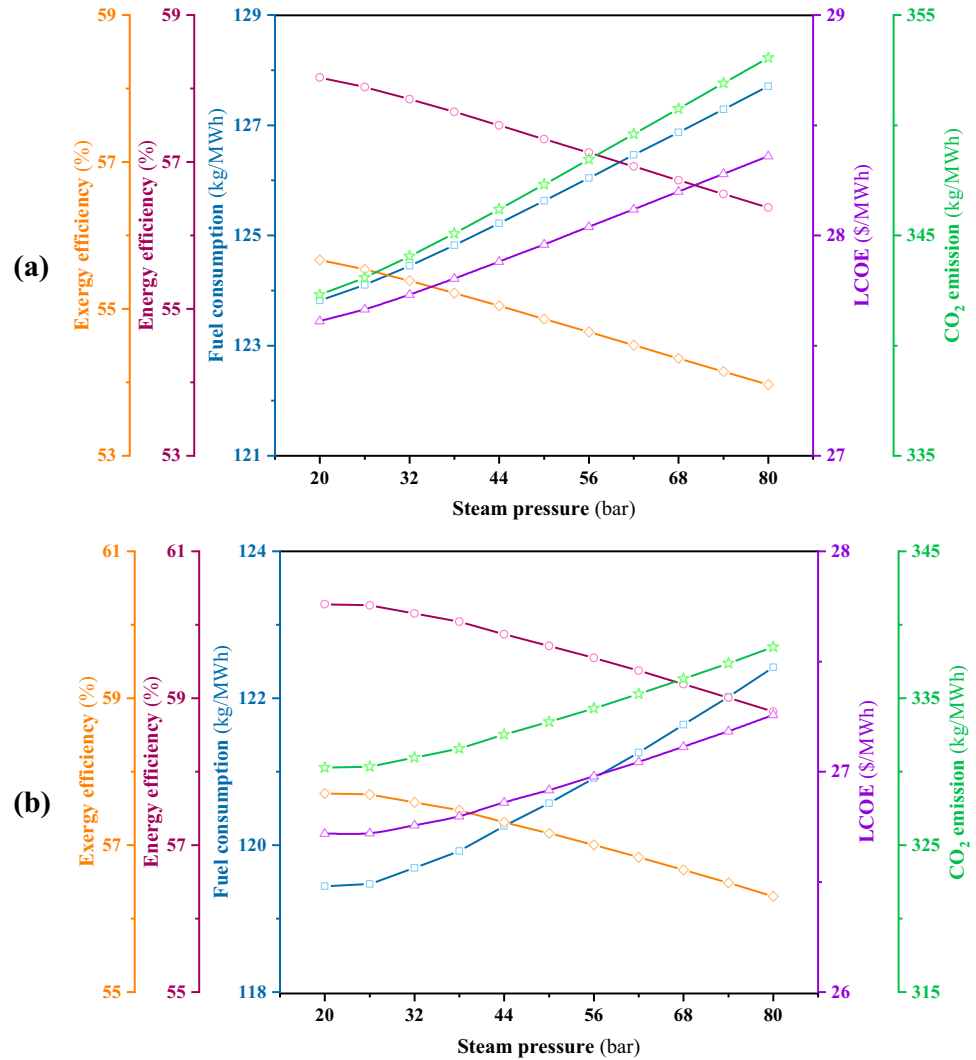
On the other hand, since the system's power is constant (40 MW), with the reduction of fuel consumption and the reduction of inlet air, the size of the equipment also decreases significantly. The amount of fuel costs also has a significant impact. As a result, the LCOE value will decrease. Figure 10 shows that the fuel consumption, CO₂ emission, and LCOE of the cycle that has used the ejector-produced refrigerant load to reduce the air temperature after the first compression is much lower than those of a system that uses an air-cooled compact heat exchanger.

The gas turbine's inlet temperature is another critical parameter affecting the BC's performance. Figure 11 shows the effect of gas turbine inlet temperature on system performance. Increasing the turbine inlet temperature from 1200 to 1600 K will reduce the fuel consumption in the proposed configuration from 150 to 114.7 kg/MWh (30.8% reduced), while it is a 25% reduction for the traditional configuration, showing a further fuel-consumption reduction in the Brayton-Rankine cycle with ejector intercooler.

Increasing TIT raises the outlet temperature of the gas turbine. As a result, the heat transfer rate in the recuperator also increases. As a result, the inlet temperature of the combustion chamber will be higher. Although more fuel is required in the combustion chamber as the inlet temperature increases, increasing the inlet temperature significantly affects the combustion chamber, increasing pressure and reducing fuel consumption. Due to the constant production capacity and fuel consumption reduction, energy efficiency and exergy will also increase.

At temperature 1400 K in the proposed configuration, the energy efficiency is 56.6%, and exergy efficiency is 54.2%, while those of the traditional configuration are 54.46 and 52.1%, respectively, concluding that the energy efficiency of configuration 2 (proposed) is about 4% higher than that of configuration 1 (used in many power plants). Nevertheless, the situation is slightly different in terms of price. Initially, with increasing TIT, fuel consumption decreases and causes

Fig. 12 Effect of steam pressure on the energetic and exergetic efficiencies, levelized cost of electricity, and levelized CO₂ emission, for the **a** traditional configuration and **b** proposed configuration



the LCOE to fall as well. However, from a temperature of 1500 K onwards, gas turbine prices increase sharply.

At 1200 K, the system LCOE is 32.94 \$/MWh, reduces to 26.97 \$/MWh at 1480 K, and after that, it has an ascending trend reaching 37.93 \$/MWh at 1600 K.

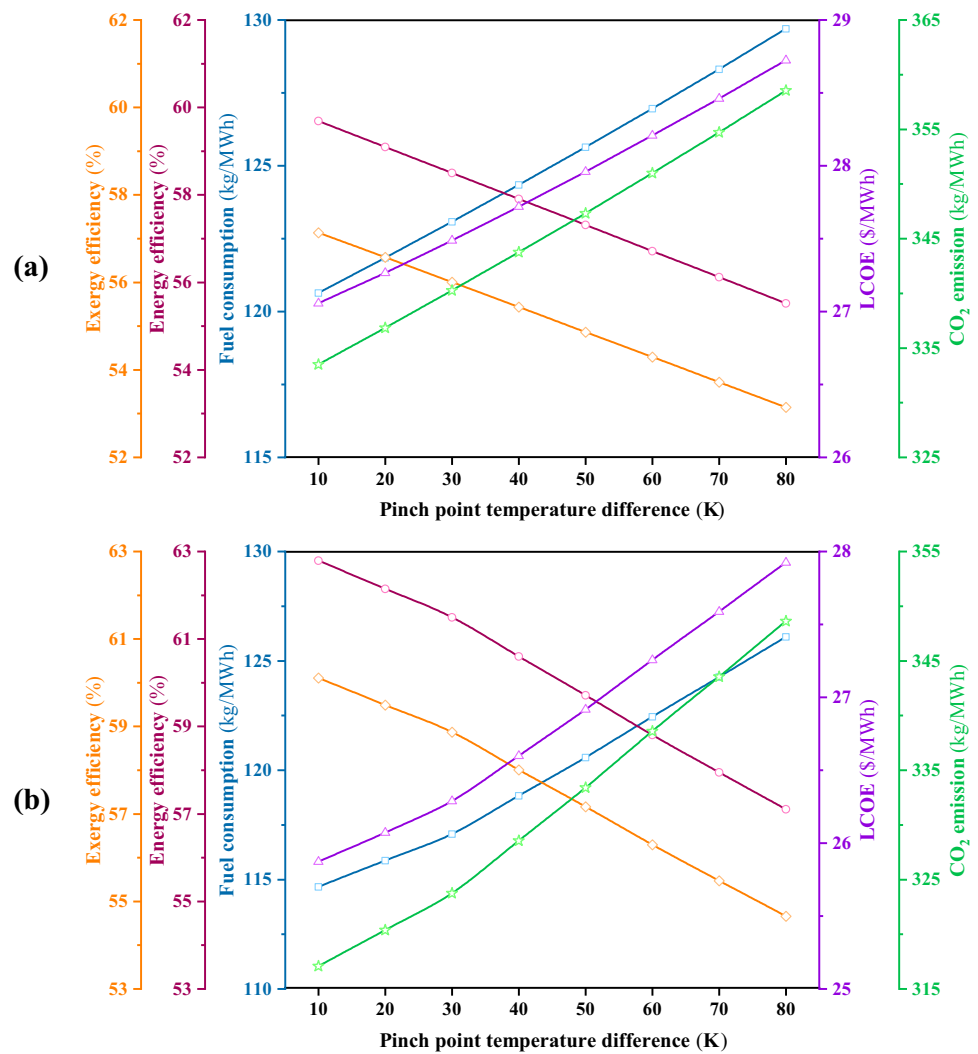
The reason is that the blades' corrosion is very high at this high temperature, and its technology is costly. As a result, temperatures above 1500 K can be unsuitable for system design.

Steam pressure has an essential effect on the performance of the HRSG and RC. The changes in the steam pressure result in saturation temperature variation, and finally, it significantly affects the heat transfer rate. The effects of steam pressure on the defined performance criteria of the system are plotted in Fig. 12. It should be noted that variation of the steam pressure has no effect on the performance of the BC, and it affects the output of the RC; hence it affects the performance of the combined cycle. As shown in Fig. 12, the fuel consumption increases as the steam pressure rises.

The reason is that increasing the steam pressure and, consequently, the heat transfer in the HRSG is reduced by increasing the steam pressure and, consequently, the saturated steam temperature. Although the pressure difference between the two sides of the steam turbine has increased, the amount of turbine power is expected to increase. Still, due to the reduced heat transfer, the amount of produced steam is significantly reduced, and its effect is more remarkable than raising the pressure difference. As a result, the power generation capacity in the steam turbine is reduced. Due to the constant generated power of the combined cycle and the reduction in output power of the RC, the fuel consumption must be increased to compensate for the RC power reduction caused by the BC; consequently, the increment in fuel consumption results in a reduction of energy and exergy efficiencies.

A point worth noting is that in the proposed configuration, the fuel consumption at the highest steam pressure is 122.4 kg/MWh, which is lower than that at the most

Fig. 13 Effect of pinch point temperature difference on the energetic and exergetic efficiencies, levelized cost of electricity, and levelized CO₂ emission, for the **a** traditional configuration and **b** proposed configuration



downward pressure in configuration 1 (124 kg/MWh). Results show that at a steam pressure of 20 bar, the proposed configuration's fuel consumption is less than that of the traditional composition, and the highest efficiency for configurations 1(traditional) and 2 (proposed) are, respectively, 58.15% and 60.28% for energy efficiency and 55.67% and 57.71% for exergy efficiency. The proposed configuration produced less CO₂ and LCOE than the traditional configuration; at a steam pressure of 20 bar, replacing the proposed configuration with the traditional configuration reduced the LCOE by 3.9%.

The pinch point temperature difference is one of the most important factors in the design of heat exchangers. This parameter determines the minimum temperature in the heat exchanger between the hot and cold flow. The lower this parameter, the higher the heat transfer and the higher the heat transfer area. Hence, a larger heat exchanger is required. Figure 13 illustrates the system performance variation by changing the pinch point temperature difference. As the HRSG is the junction of the BC and RC, its performance

dramatically affects the entire system's performance. Based on Fig. 13, the fuel consumption rises as the pinch point increases.

Results show that an increase in the proposed configuration's pinch-point temperature from 20 to 80 °C will increase the fuel consumption by 8.6%, causing the energy and exergy efficiencies to drop by 8.11 and 8%, respectively.

Increasing the pinch point reduces the heat transfer in HRSG, reducing the steam flow rate. As the amount of steam decreases, the power output of the steam turbine is also reduced. As a result, fuel consumption increases due to the constant power output. As fuel consumption increases, energy and exergy efficiencies are also decreased. Increasing fuel consumption also increases the production of pollutants and LCOE.

Comparing the results at a pinch-point temperature of 20 °C reveals that the fuel consumption, CO₂ emission, and LCOE in the proposed configuration have been reduced by 4.92%, 5% and 4.76% compared to the traditional configuration. Regarding the energy and exergy efficiencies,

Fig. 14 Effect of steam turbine inlet temperature on the energetic and exergetic efficiencies, leveled cost of electricity, and leveled CO₂ emission, for the **a** traditional configuration and **b** proposed configuration

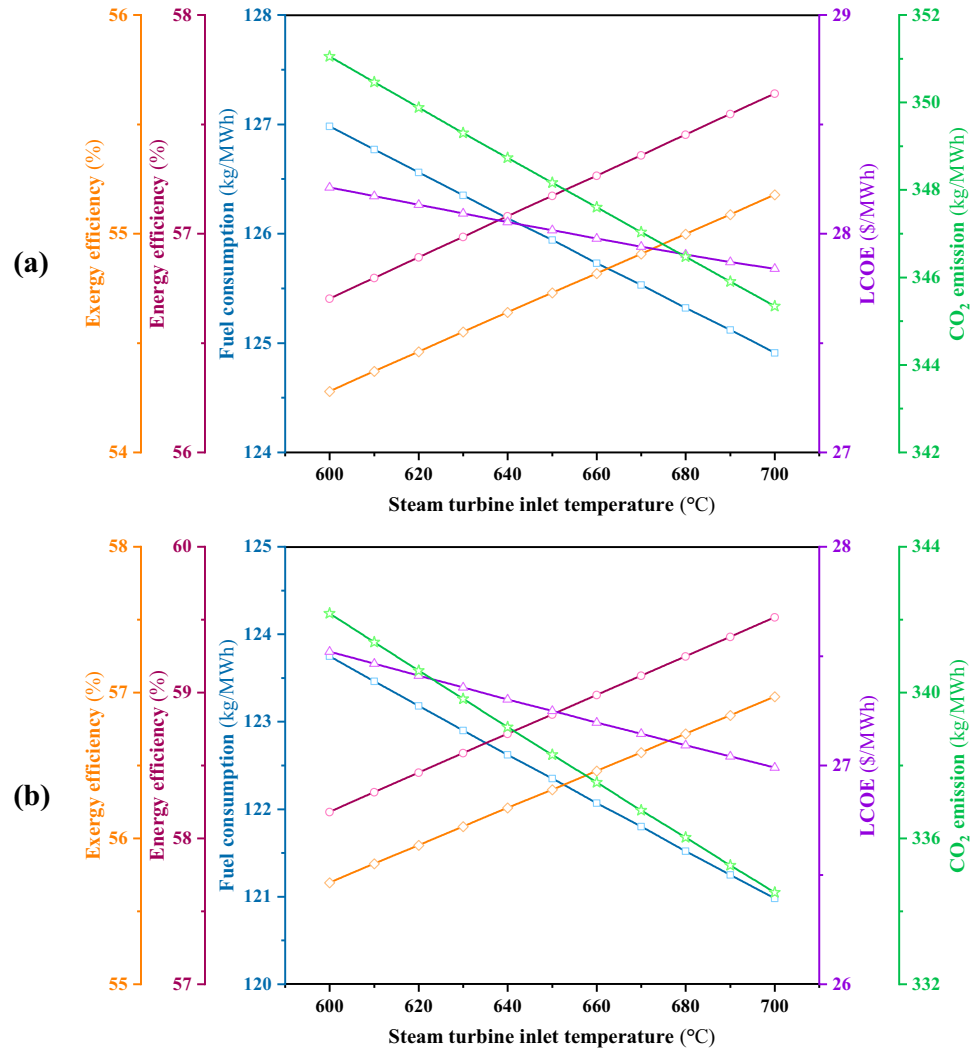


Table 10 Ranking of the most influential parameters on the performance of the two designs

Rank	Parameter	Range	Optimum value	Design	Sensitivity				
					ΔFC (kg/MWh)	$\Delta \eta_{energy}$ (%)	$\Delta \eta_{exergy}$ (%)	$\Delta LCOE$ (\$/MWh)	ΔCO_2 (kg/MWh)
1	Pressure ratio	2–16	16	(1)	36	13.1	12.6	6.8	100.8
				(2)	47.4	18	7.2	8.9	131.2
2	Gas turbine inlet temperature	1200–1600 K	For LCOE: 1520 K Others: 1600 K	(1)	35.1	13.5	3.1	11.2	98.4
				(2)	35.3	15	4.3	10.9	98.4
3	Pinch point temperature difference	20–80 °C	20 °C	(1)	8	3.6	3.5	2.208	33.01
				(2)	10.2	5.1	4.9	2.75	42.2
4	Steam pressure	20–80 bar	20 bar	(1)	3.8	1.79	1.8	0.4	7.3
				(2)	2.9	1.5	1.4	0.3	5.1
5	Steam turbine inlet temperature	600–700 °C	700 °C	(1)	2.1	0.9	0.9	0.4	5.8
				(2)	2.7	1.4	1.3	0.6	7.8

the enhancements at this temperature are 5.4% and 5.31%, respectively, in the proposed configuration compared to the traditional configuration.

Figure 14 shows the impact of steam turbine inlet temperature on the 4E criteria of the proposed combined system. Results show that at 700 °C inlet temperature of the steam turbine, the energy and exergy efficiencies of the proposed configuration, which uses the ejector refrigeration cycle as an intercooler, are 59.52% and 56.97%, respectively. When the temperature increases from 600 to 700 °C, the fuel consumption drops from 124 to 121 kg/MWh.

As inferred from this figure, higher steam turbine inlet temperature leads to higher system efficiency and lower fuel consumption. Accordingly, the CO₂ emission and LCOE of the combined cycle reduce with increasing steam turbine inlet temperature.

Based on the results, the LCOE and CO₂ emissions are less in the proposed configuration than in the traditional conclusion. At a 650 °C steam turbine inlet temperature, the former is 27.25 \$/MWh, and the latter is 338 kg/MWh in the proposed configuration, while they are 28.01 \$/MWh and 348 kg/MWh in a traditional configuration, which uses a compact heat exchanger as an intercooler in the Brayton-Rankine cycle. It shows that using the ejector refrigeration cycle as an intercooler not only affects the energy and exergy efficiencies positively but also has environmental and economic advantages.

The parametric study results have been summarized in Table 10 to compare the effects of different parameters better. All the parameters that are studied are ranked based on the sensitivity analysis for the two proposed configurations

[expressed as design (1-traditional configuration) and (2-proposed configuration) in Table 10]. The most influential parameter is the compressor pressure ratio, with a rank of 1, and the least effective one is the steam turbine inlet temperature, with a rank of 5. The parametric study results in Table 10 also attest that the combined system with the ERC intercooler performs better than the combined system with the air-cooled intercooler in most cases.

The optimum value of the system performance is presented as the final results. The Pareto optimal frontier of the two considered optimization objective functions (exergy efficiency and levelized cost of electricity) is depicted in Fig. 15. Despite single-objective optimization problems that have a certain value as the “optimal solution”, the multi-objective optimization problem has a set of optimal solutions (the Pareto optimal frontier) that do not dominate each other. Each point in Fig. 15 could be considered an optimum solution candidate. Among all these optimum points, the designer should be selected one point based on a decision-making method. The LINMAP (Khanmohammadi and Musharavati 2021) decision-making method is utilized to choose the best point. This method is based on the lowest normalized distance from the ideal point (the ideal point is an unreal point in which both objective functions are simultaneously in their best possible value).

Applying the abovementioned process, point B is the final optimal point. The values of the objective functions are obtained as $\eta_{ex,opt} = 57.64\%$, and $LCOE_{opt} = 29.93$ \$/MWh at this point. These values have occurred at the optimal operating conditions of $PR_{opt} = 12.77$, $T_{GT,opt} = 1544.19$ K, $P_{st,opt} = 19.82$ bar, $\Delta T_{PP,opt} = 10.06$ K, and $T_{ST,opt} = 682.11$ K. Furthermore, as a practical optimization finding, a curve is fitted on the Pareto frontier points, and its correlation is obtained (Eq. (19)). Using this correlation, the designer can access their desirable optimal system performance based on this proposed CCHP system.

$$\eta_{ex,opt} = -0.0032(LCOE_{opt})^3 + 0.2612(LCOE_{opt})^2 - 6.5085(LCOE_{opt}) + 103.63 \tag{19}$$

6 Conclusions

The present study developed a novel combination of an ejector refrigerating cycle with a Brayton-Rankine power cycle to recover the wasted heat of the boiler to produce a refrigerating load to reuse an intercooler between the compressing stages in the Brayton cycle. Earlier investigations studied the feasibility of producing refrigerating loads from the recovering wasted heat of the Brayton-Rankine power cycles by combining them

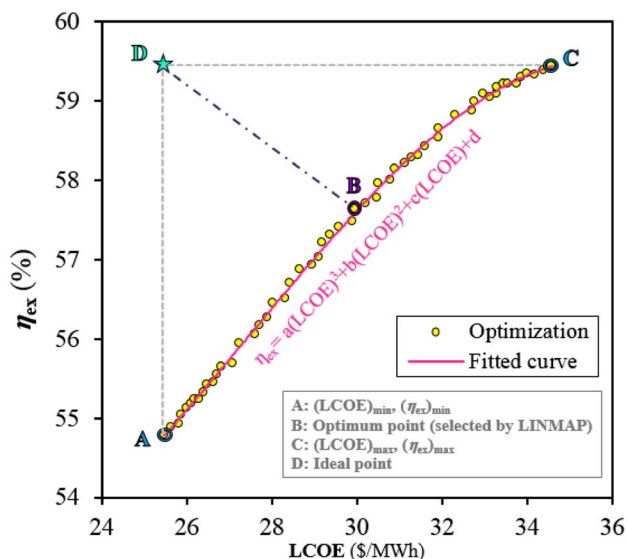


Fig. 15 The Pareto optimal frontier and the selected optimum point with the LINMAP method

with an ejector refrigerating cycle for external utilization. However, it is aimed to be used as the intercooling of the primary Brayton cycle, which has been proposed in this paper for the first time. A 4E-analysis including energy, exergy, economics, and environmental analyses have been performed to investigate the proposed combination of the Brayton-Rankine cycle with the ejector refrigerating cycle and compare it with traditional types of Brayton-Rankine cycles. Finally, a parametric study and an optimization model are also developed to evaluate the proposed ERC-Brayton-Rankine cycle performance and find its optimal operating point using the NSGA-II method. The main conclusions of the analyses could be summarized as follows:

- Comparing the results of the first and second configurations of the combined cycle with their corresponding base cycle showed that the fuel consumption was reduced by 7.61% and 13.47% using the first and second combined cycles, respectively. It led to significant cost savings. Also, comparing the energy efficiencies resulted in 8.25% and 15.47% increments using the combined process instead of the basic cycle with the first and second intercooling approaches, respectively.
- The results also indicated that although the ERC intercooler may cause a slight reduction (about 2.4%) in the energy and exergy efficiencies compared to air-cooled intercooler in the BC, however, because the turbine exhaust temperature is higher when the ERC intercooler was used, therefore in case of integrated approach the opposite was true. The combined system with the ERC intercooler yielded a 4% increment in efficiencies concerning the air-cooled intercooler.
- In a combined system, the highest exergy destruction occurred within the BC, about 92.2% for the air-cooled and 82.1% for the ERC intercooler. The combustion chamber played the most significant role in exergy destruction in BC. Conversely, using the ERC intercooler instead of the air-cooled type could reduce the heat recovery steam generator (HRSG) exergy destruction in the RC by 36.5%.
- The results of the economics analysis showed that most of the capital cost was dedicated to the upstream cycle (i.e., BC). The outcomes of the economic analysis also illustrated that most of the capital cost of both BC and RC goes to the turbines. It was while the main capital cost after the turbine belongs to the ERC due to the costs of the generator and condenser.
- The parametric study results revealed that the most influential parameter on the performance criteria of the system was the compressor pressure ratio, and the steam turbine inlet temperature was the least effective parameter. These sensitivity parameter analysis results are beneficial for optimizing all the effective parameters so that some of

the desired cost functions, such as specific fuel consumption/LCOE/CO₂ emissions minimization or energy and exergy efficiencies maximization, are optimized.

- Considering the exergetic efficiency and leveled cost of electricity as two objective optimization functions in a multi-criteria NSGA-II optimization procedure resulted in the optimum values of $\eta_{ex,opt} = 57.64\%$ and $LCOE_{opt} = 29.93 \text{ \$/MWh}$.

References

- Ahmadi P, Dincer I (2010) Exergoenvironmental analysis and optimization of a cogeneration plant system using multimodal genetic algorithm (MGA). *Energy* 35(12):5161–5172. <https://doi.org/10.1016/j.energy.2010.07.050>
- Ahmadi P, Rosen MA, Dincer I (2011) Greenhouse gas emission and exergo-environmental analyses of a trigeneration energy system. *Int J Greenh Gas Control* 5:1540–1549. <https://doi.org/10.1016/j.ijggc.2011.08.011>
- Ahmadzadeh A, Salimpour MR, Sedaghat A (2017) Thermal and exergoeconomic analysis of a novel solar driven combined power and ejector refrigeration (CPER) system. *Int J Refrig* 83:143–156. <https://doi.org/10.1016/j.ijrefrig.2017.07.015>
- Alexis GK (2007) Performance parameters for the design of a combined refrigeration and electrical power cogeneration system. *Int J Refrig* 30:1097–1103. <https://doi.org/10.1016/j.ijrefrig.2006.12.013>
- Alirahmi SM, Rahmani Dabbagh S, Ahmadi P, Wongwises S (2020) Multi-objective design optimization of a multi-generation energy system based on geothermal and solar energy. *Energy Convers Manag* 205:112426. <https://doi.org/10.1016/j.enconman.2019.112426>
- Ameri M, Behbahania A, Tanha AA (2010) Thermodynamic analysis of a tri-generation system based on micro-gas turbine with a steam ejector refrigeration system. *Energy* 35:2203–2209. <https://doi.org/10.1016/j.energy.2010.02.006>
- Anvari S, Mahian O, Taghavifar H, Wongwises S, Desideri U (2020) 4E analysis of a modified multi-generation system designed for power, heating/cooling, and water desalination. *Appl Energy* 270:115107. <https://doi.org/10.1016/j.apenergy.2020.115107>
- Bejan A, Tsatsaronis G, Moran M (1996) *Thermal design and optimization*. Wiley, Hoboken
- Cengel YA, Boles MA (2006) *Thermodynamics: an engineering approach*, 5th edn. McGraw Hill, New York
- Dai Y, Wang J, Gao L (2009) Exergy analysis, parametric analysis and optimization for a novel combined power and ejector refrigeration cycle. *Appl Therm Eng* 29:1983–1990. <https://doi.org/10.1016/j.applthermaleng.2008.09.016>
- Dang W, Liao S, Yang B, Yin Z, Liu M, Yin L, Zheng W (2023) An encoder-decoder fusion battery life prediction method based on Gaussian process regression and improvement. *J Energy Storage* 59:106469. <https://doi.org/10.1016/j.est.2022.106469>
- Dincer I, Rosen MA (2007) *Exergy: energy, environment and sustainable development*. Elsevier, Amsterdam
- Durmusoglu Y, Ust Y, Kayadelen HK (2017) Thermoeconomic optimization and performance analysis of a regenerative closed brayton cycle with internal irreversibilities and pressure losses. *Iran J Sci Technol Trans Mech Eng* 41:61–70. <https://doi.org/10.1007/s40997-016-0043-3>
- Ebrahimi-Moghadam A, Farzaneh-Gord M (2021) Energy, exergy, and eco-environment modeling of proton exchange membrane

- electrolyzer coupled with power cycles: application in natural gas pressure reduction stations. *J Power Sources* 512:230490. <https://doi.org/10.1016/j.jpowsour.2021.230490>
- Ebrahimi-Moghadam A, Farzaneh-Gord M (2023) A sustainable optimal biomass waste-driven CCHP system to boost the nearly zero energy building concept. *Energy Convers Manag* 277:116669. <https://doi.org/10.1016/j.enconman.2023.116669>
- Farmani A, Manjili FE (2022) Power generation improvement of gas turbines in hot seasons by injecting compressed air through an external compressor. *Iran J Sci Technol Trans Mech Eng* 46:817–828. <https://doi.org/10.1007/s40997-022-00515-y>
- Galindo J, Dolz V, Tiseira A, Ponce-Mora A (2019) Thermodynamic analysis and optimization of a jet ejector refrigeration cycle used to cool down the intake air in an IC engine. *Int J Refrig* 103:253–263. <https://doi.org/10.1016/j.jrefrig.2019.04.019>
- Gas Turbine Emissions (2013) Cambridge aerospace series. Cambridge University Press, Cambridge. <https://doi.org/10.1017/CBO9781139015462>
- Ge L, Du T, Li C, Li Y, Yan J, Rafiq MU (2022) Virtual collection for distributed photovoltaic data: challenges, methodologies, and applications. *Energies*. <https://doi.org/10.3390/en15238783>
- Ghadikolaei RS, Khoshgoftar Manesh MH, Modabber HV, Onishi VC (2023) Thermo-environ-economic optimization of an integrated combined-cycle power plant based on a multi-objective water cycle algorithm. *Iran J Sci Technol Trans Mech Eng*. <https://doi.org/10.1007/s40997-023-00668-4>
- Golbaten Mofrad K, Zandi S, Salehi G, Khoshgoftar Manesh MH (2020) 4E analyses and multi-objective optimization of cascade refrigeration cycles with heat recovery system. *Therm Sci Eng Prog* 19:100613. <https://doi.org/10.1016/j.tsep.2020.100613>
- Gu Q, Tian J, Yang B, Liu M, Gu B, Yin Z, Yin L, Zheng W (2023) A novel architecture of a six degrees of freedom parallel platform. *Electronics*. <https://doi.org/10.3390/electronics12081774>
- Gülen SC, Rogers J, Sprengel M (2020) DICE-gas turbine compound reheat combined cycle. *Fuel* 279:118515. <https://doi.org/10.1016/j.fuel.2020.118515>
- Haloi P, Gogoi TK (2022) Effects of partially ionized combustion products on the performance of a magneto-hydrodynamics (MHD)-gas turbine (GT) combined power plant, part I: exergy analysis. *Iran J Sci Technol Trans Mech Eng* 46:481–495. <https://doi.org/10.1007/s40997-021-00456-y>
- He WF, Dai YP, Wang JF, Li MQ, Ma QZ (2013) Performance prediction of an air-cooled steam condenser using UDF method. *Appl Therm Eng* 50:1339–1350. <https://doi.org/10.1016/j.applthermaleng.2012.06.020>
- Hosseini M, Dincer I, Ahmadi P, Avval HB, Ziaasharhagh M (2013) Thermodynamic modelling of an integrated solid oxide fuel cell and micro gas turbine system for desalination purposes. *Int J Energy Res* 37:426–434. <https://doi.org/10.1002/er.1945>
- Kakkirala V, Velayudhan Parvathy C (2022) Optimized mixing chamber length and diameter of a steam ejector for the application of gas turbine power plant: a computational approach. *J Therm Anal Calorim* 147:8881–8894. <https://doi.org/10.1007/s10973-021-11190-7>
- Karimi MH, Chitgar N, Emadi MA, Ahmadi P, Rosen MA (2020) Performance assessment and optimization of a biomass-based solid oxide fuel cell and micro gas turbine system integrated with an organic Rankine cycle. *Int J Hydrog Energy* 45:6262–6277. <https://doi.org/10.1016/j.ijhydene.2019.12.143>
- Kays WM, London AL (1984) Compact heat exchangers. McGraw-Hill, New York
- Khanmohammadi S, Musharavati F (2021) Multi-generation energy system based on geothermal source to produce power, cooling, heating, and fresh water: exergoeconomic analysis and optimum selection by LINMAP method. *Appl Therm Eng* 195:117127. <https://doi.org/10.1016/j.applthermaleng.2021.117127>
- Kialashaki Y (2018) A linear programming optimization model for optimal operation strategy design and sizing of the CCHP systems. *Energy Effic* 11:225–238. <https://doi.org/10.1007/s12053-017-9560-1>
- Kilani N, Khir T, Ben Brahim A (2019) Energetic and exergetic optimization of a combined cycle power plant with dual-pressure HRSG, compressed air cooling, steam injection and vapor extraction systems. *Iran J Sci Technol Trans Mech Eng* 43:527–536. <https://doi.org/10.1007/s40997-018-0175-8>
- Lemmon E, Huber M, McLinden M (2010) NIST standard reference database 23, reference fluid thermodynamic and transport properties (REFPROP), Version 9.0. National Institute of Standards and Technology
- Li X, Wang N, Wang L, Kantor I, Robineau J-L, Yang Y, Maréchal F (2018) A data-driven model for the air-cooling condenser of thermal power plants based on data reconciliation and support vector regression. *Appl Therm Eng* 129:1496–1507. <https://doi.org/10.1016/j.applthermaleng.2017.10.103>
- Liang Y, Sun Z, Dong M, Lu J, Yu Z (2020) Investigation of a refrigeration system based on combined supercritical CO₂ power and transcritical CO₂ refrigeration cycles by waste heat recovery of engine. *Int J Refrig* 118:470–482. <https://doi.org/10.1016/j.jrefrig.2020.04.031>
- Mahmoudan A, Esmailion F, Hoseinzadeh S, Soltani M, Ahmadi P, Rosen M (2022) A geothermal and solar-based multi-generation system integrated with a TEG unit: Development, 3E analyses, and multi-objective optimization. *Appl Energy* 308:118399. <https://doi.org/10.1016/j.apenergy.2021.118399>
- Moghimi M, Emadi M, Ahmadi P, Moghadasi H (2018) 4E analysis and multi-objective optimization of a CCHP cycle based on gas turbine and ejector refrigeration. *Appl Therm Eng* 141:516–530. <https://doi.org/10.1016/j.applthermaleng.2018.05.075>
- Mohammadi A, Kasaeian A, Pourfayaz F, Ahmadi MH (2017) Thermodynamic analysis of a combined gas turbine, ORC cycle and absorption refrigeration for a CCHP system. *Appl Therm Eng* 111:397–406. <https://doi.org/10.1016/j.applthermaleng.2016.09.098>
- Mohammadi K, McGowan JG, Saghafifar M (2019) Thermo-economic analysis of multi-stage recuperative Brayton power cycles: Part I-hybridization with a solar power tower system. *Energy Convers Manag* 185:898–919. <https://doi.org/10.1016/j.enconman.2019.02.012>
- Mohammed RH, Qasem NAA, Zubair SM (2022) Exergoeconomic optimization of an integrated supercritical CO₂ power plant and ejector-based refrigeration system for electricity and cooling production. *Arab J Sci Eng* 47:9137–9149. <https://doi.org/10.1007/s13369-021-06414-9>
- Musharavati F, Khanmohammadi S, Pakseresht A, Khanmohammadi S (2021) Waste heat recovery in an intercooled gas turbine system: Exergo-economic analysis, triple objective optimization, and optimum state selection. *J Clean Prod* 279:123428. <https://doi.org/10.1016/j.jclepro.2020.123428>
- Raghavendra H, Suryanarayana Raju P, Hemachandra Reddy K (2022) Effect of geometric and operational parameters on the performance of a beta-type stirling engine: a numerical study. *Iran J Sci Technol Trans Mech Eng* 46:1–13. <https://doi.org/10.1007/s40997-020-00406-0>
- Saidi A., Sundén, B., Eriksson, D., (2000) Intercoolers in gas turbine systems and combi-processes for production of electricity. <https://doi.org/10.1115/2000-GT-0234>
- Saidi A, Eriksson D, Sundén B (2002) Analysis of some heat exchanger concepts for use as gas turbine intercoolers
- Sanjay (2011) Investigation of effect of variation of cycle parameters on thermodynamic performance of gas-steam combined cycle. *Energy* 36:157–167. <https://doi.org/10.1016/j.energy.2010.10.058>

- Schall D, Hirzel S (2012) Thermal cooling using low-temperature waste heat: a cost-effective way for industrial companies to improve energy efficiency? *Energy Effic* 5:547–569. <https://doi.org/10.1007/s12053-012-9151-0>
- Schobeiri MT (2018) Gas turbine design, components and system design integration, 1st edn. Springer International Publishing. <https://doi.org/10.1007/978-3-319-58378-5>
- Seyfouri Z, Ameri M, Mehrabian MA (2022) Energy, exergy and economic analyses of different configurations for a combined HGAX/ORC cooling system. *Iran J Sci Technol Trans Mech Eng* 46:733–744. <https://doi.org/10.1007/s40997-022-00497-x>
- Sheykhi M, Chahartaghi M, Hashemian SM (2020) Performance evaluation of a combined heat and power system with stirling engine for residential applications. *Iran J Sci Technol Trans Mech Eng* 44:975–984. <https://doi.org/10.1007/s40997-019-00303-1>
- Sun F, Fu L, Sun J, Zhang S (2014) A new waste heat district heating system with combined heat and power (CHP) based on ejector heat exchangers and absorption heat pumps. *Energy* 69:516–524. <https://doi.org/10.1016/j.energy.2014.03.044>
- Takleh HR, Zare V (2021) Proposal and thermoeconomic evaluation with reliability considerations of geothermal driven trigeneration systems with independent operations for summer and winter. *Int J Refrig*. <https://doi.org/10.1016/j.ijrefrig.2020.12.033>
- Tozlu A, Abusoglu A, Ozahi E, Anvari-Moghaddam A (2021) Municipal solid waste-based district heating and electricity production: A case study. *J Clean Prod* 297:126495. <https://doi.org/10.1016/j.jclepro.2021.126495>
- Tyagi SK, Chen GM, Wang Q, Kaushik SC (2006) Thermodynamic analysis and parametric study of an irreversible regenerative-intercooled-reheat Brayton cycle. *Int J Therm Sci* 45:829–840. <https://doi.org/10.1016/j.ijthermalsci.2005.10.011>
- Valero A, Lozano MA, Serra L, Tsatsaronis G, Pisa J, Frangopoulos C, von Spakovsky MR (1994) CGAM problem: definition and conventional solution. *Energy* 19:279–286. [https://doi.org/10.1016/0360-5442\(94\)90112-0](https://doi.org/10.1016/0360-5442(94)90112-0)
- Vazini Modabber H, Khoshgoftar Manesh MH (2021) 4E dynamic analysis of a water-power cogeneration plant integrated with solar parabolic trough collector and absorption chiller. *Therm Sci Eng Prog* 21:100785. <https://doi.org/10.1016/j.tsep.2020.100785>
- Vutukuru R, Pegallapati AS, Maddali R (2019) Thermodynamic studies on a solar assisted transcritical CO₂ based tri-generation system with an ejector for dairy applications. *Int J Refrig* 108:113–123. <https://doi.org/10.1016/j.ijrefrig.2019.08.031>
- Wang Z, Han W, Zhang N, Su B, Gan Z, Jin H (2018) Effects of different alternative control methods for gas turbine on the off-design performance of a trigeneration system. *Appl Energy* 215:227–236. <https://doi.org/10.1016/j.apenergy.2018.01.053>
- Wang A, Wang S, Ebrahimi-Moghadam A, Farzaneh-Gord M, Moghadam AJ (2022) Techno-economic and techno-environmental assessment and multi-objective optimization of a new CCHP system based on waste heat recovery from regenerative Brayton cycle. *Energy* 241:122521. <https://doi.org/10.1016/j.energy.2021.122521>
- Wang Z, Chen H, Xia R, Han F, Ji Y, Cai W (2022) Energy, exergy and economy (3E) investigation of a SOFC-GT-ORC waste heat recovery system for green power ships. *Therm Sci Eng Prog* 32:101342. <https://doi.org/10.1016/j.tsep.2022.101342>
- Wang J, Tian J, Zhang X, Yang B, Liu S, Yin L, Zheng W (2022b) Control of time delay force feedback teleoperation system with finite time convergence. *Front Neurobot* <https://doi.org/10.3389/fnbot.2022.877069>
- Wu C, Chen L, Sun F (1996) Performance of a regenerative Brayton heat engine. *Energy* 21:71–76. [https://doi.org/10.1016/0360-5442\(95\)00097-6](https://doi.org/10.1016/0360-5442(95)00097-6)
- Xu XX, Liu C, Fu X, Gao H, Li Y (2015) Energy and exergy analyses of a modified combined cooling, heating, and power system using supercritical CO₂. *Energy* 86:414–422. <https://doi.org/10.1016/j.energy.2015.04.043>
- Xu Z, Yang H, Xie Y, Zhu J, Liu C (2022) Thermodynamic analysis of a novel adiabatic compressed air energy storage system with water cycle. *J Mech Sci Technol* 36:3153–3164. <https://doi.org/10.1007/s12206-022-0546-3>
- Zhang C, Lin J, Tan Y (2021) Thermodynamic analysis of a parallel type organic rankine cycle and ejector heat pump combined cycle. *Appl Therm Eng* 182:116061. <https://doi.org/10.1016/j.applthermaleng.2020.116061>

Springer Nature or its licensor (e.g. a society or other partner) holds exclusive rights to this article under a publishing agreement with the author(s) or other rightsholder(s); author self-archiving of the accepted manuscript version of this article is solely governed by the terms of such publishing agreement and applicable law.